The authors thank the reviewers for thorough reading and comments to the manuscript. Please find responses to specific comments below.

Note: The authors added a full year of data (2017) to the updated manuscript.

Reviewer 1 comment:

The authors use additional vegetation/leaf level measurements of photosynthesis and conductance to strengthen their assertions of flux dynamics, although the discussion of these results feels rather like a tangential addition. These findings could be more strongly incorporated into the discussion of differences in fluxes from old and young leaves and into the discussion of the influence of diurnal cycles and hysteresis on seasonal trends.

[…] A more complete discussion of the old and young leaf-level data would likewise improve support for the conclusion that GPP was limited by leaf age in the summer. Following these additions, strong conclusions regarding the influence of global climate change on the future carbon exchange in these forests can be drawn.

Response:

Thank you for this suggestion. Although we lack site-specific data on leaf age effects on A_{max}, we incorporated a relevant reference to the discussion: "In Australian woodlands, PC (A_{max}) of leaves was also found to decrease with leaf age, A_{max} declined by 30% on average between young and old leaves, for 10 different species (Reich et al., 2009).", L391-393. This suggests that both leaf age and LAI are important in limiting GPP at our site.

Reviewer 1 comment:

The work of A. Griebel on anisohydricity induced by mistletoes in these ecosystems could be drawn upon in greater detail during the discussion of leaf specific measurements and trends in seasonal response to moisture availability as it is likely as highly relevant to ecosystem carbon dynamics as it is to water dynamics.

Response:

Thank you for this suggestion. We would like to include discussion of the effects of biotic disturbance by mistletoe at our site, but these data are not yet publicly available. Moreover, detailed leaf-level responses are beyond the scope of this manuscript.

Reviewer 1 comment:

The authors conclude that diurnal patterns of NEE, GPP, and ER have central roles in determining the seasonal carbon source/sink dynamics, but a stronger analysis would significantly bolster this claim – a wavelet coherence analysis of the time series could be an informative addition that would support this conclusion more thoroughly.

Response:

Thank you for this suggestion. We conducted a wavelet coherence analysis to assess the coherence between GPP and D (figure S11). We did not add the figure to the main text, as the observed coherence between GPP and D is mostly due to daily cycle (GPP and D high during the day, low during night) and annual cycle (GPP and D high in summer, low in winter). Moreover, D covaries with other drivers such as PPFD and Ta, which makes it difficult to attribute coherence solely to D. Some interesting coherence appeared at weekly and monthly period. Furthermore, wavelet coherence is useful to quantify phase lags, but this is beyond the scope of the current manuscript.

Reviewer 1 comment:

Lastly, while this paper makes a significant contribution without it, an analysis of GPP in comparison to solar induced fluorescence (SIF) which has been recently shown as a better proxy for GPP than NDVI may prove very interesting.

Response:

Thank you for this suggestion. We note that EVI was better than NDVI for predicting PC and canopy conductance at our site. However, SIF analysis is beyond the scope of our work.

Reviewer 1 comment:

L243: Were leaves actually measured at 1.5km height as this sentence suggests? From what light environment were measured leaves collected?

Response:

Thank you for pointing out the typo. We also removed the detailed of leaf gas exchange measurement from section 2.13, L256-258, as we used previously published data.

Reviewer 2 comment:

Please eliminate the use of the diffusely defined term "atmospheric drought". A term like "atmospheric demand" is more precise and appropriate.

Response:

Amended. L30, 33, 67, 307, 341, 372 and 462

Reviewer 2 comment:

Is it really true that the canopy height is ~25 m (L105) and the top of the profile and eddy covariance system is 29 m? This is rather close to a tall canopy for an eddy covariance application for observing ecosystem fluxes. A check of the site description is needed, and if indeed these numbers correct, a clearer presentation and discussion of the implications on representativeness of reported fluxes and analyses is in order.

Response:

We agree that our initial statement was misleading, so we used airborne LiDAR data to inspect the structural canopy properties within the footprint of the flux tower and have done an analysis of the cospectra of w and CO_2 to assess any influence of the instrument height above the canopy on the turbulent transport characteristics (figure S3). We added a figure that summarizes the canopy structure as a height profile of the frequency of LiDAR returns to the supplements (figure S1) and amended the canopy description in section 2.1, L101-109, as follows:

"The flux tower is in a mature dry sclerophyll forest, with 140 Mg C ha^{-1} aboveground biomass and stand density of ~500 trees ha^{-1}. The stand hosts a large population of mistletoe (*Amyema miquelii*), which is decreasing in abundance with increasing distance to the flux tower. The canopy structure comprises three strata, and the predominant canopy tree species are *Eucalyptus moluccana* and *E. fibrosa*. While individual trees can exceed 25 m height, an airborne LiDAR survey from November 2015 indicates an average canopy height of ~24 m within a 300 m radius of the flux tower (supplement figure S1). The mid-canopy stratum (5-12 m) is dominated by *Melaleuca decora* and the understory is dominated by *Bursaria spinosa* with various shrubs, forbs, grasses and ferns present in lower abundance."

Also, we added more details regarding the turbulent fluxes quality in the section 2.4, L163-165

"Although the tower height (29m) is rather close to the average canopy height (24m), cospectra analysis showed good quality turbulent fluxes (the high frequency followed the -4/3 slope, thus we did not find any indications of systematic dampening in the cospectra, see figure S3)."

Reviewer 2 comment:

Was NDVI measured at the site or was a satellite product used? What was the rationale for using only NDVI versus EVI (or checking both)?

Response:

We used LANDSAT satellite products. We replaced NDVI with EVI in the main document, as it appeared to be more closely related to canopy dynamics at the site, and moved NDVI to the supplements (see figure 1, figure 6 and figure S9, EVI follows LAI time dynamic and is better correlated with PC and $G_{s,max}$). We thank the reviewer for this useful observation.

Reviewer 2 comment:

A careful read and editing of the methods (and entire manuscript) is needed to ensure better consistency in the use of terminology and symbols be used. Furthermore, where possible, the use of more common symbols/abbreviations would be helpful. A non-exhaustive list of examples includes:

- F_{CT} and F_{CS} are used to represent the eddy flux and storage flux, respectively (Eq. 1). Then F_c and S_c are used to represent the eddy flux and storage flux, respectively (L136).
- F_N (e.g., L183-184) and R_n (L196) are used alternately to represent net radiation.
- The profile system measured CO_2 "mixing ratios" (L115), then "concentration" is used later (L160-170) with a symbol similar to the "concentrations" referred to in relation to the high frequency density measurements made by the open path IRGA.
- Use Δ or s for the slope of the saturation vapor pressure curve instead of ε
- Use LE or λE for latent heat flux

Response:

We have revised the manuscript and improved the consistency of terminology throughout.

- F_c and S_c → F_{CT} and F_{CS}, L134
- F_n → R_n, L197, L210, L218
- More precision added: CO_2 is measured in ppm and converted to µmol m^{-3} using ideal gas law equation. L171-172
- Equation (4), equation (6), L218, ε → Δ
- Equation (4), L217, latent heat flux L → λE
- Equation (5), L221, U → w_s

Reviewer 2 comment:

The sign conventions regarding the directions of fluxes are mixed up in places. For example, in the abstract C sinks carry a positive sign for uptake (L18-19), but later in the text (L264-265) "C sinks" are reported with negative signs. Please carefully review the entire manuscript and ensure consistency throughout regarding sign conventions for fluxes, sinks, and sources.

Response:

We have consistently adopted the usual convention from micro-meteorology, that is C going out of the atmosphere is negative (uptake), and C going into the atmosphere is positive (source). L18

Reviewer 2 comment:

L111…The LI190SB quantum sensor is calibrated to report PPFD as µmol/m^2/s. Was this then converted to W/m^2? Check the units throughout the manuscript because the reported values for incident PAR in W/m^2 (e.g., L230-231 and 242, Figs. 1 and 3) are not physically possible. Also check to ensure that there was no effect on analyses and it is only an error in the manuscript text.

Response:

There was an error in the manuscript text; PPFD is measured in µmol m^{-2} s^{-1}. This has been corrected throughout the text, equations and figures. L83, 113, 235, 239, 245, 247, 252, 263, 309, 310, 320, 361, 362, 440, 442, 457, 464, 465, 472 and 479, figure 1, 3, 4 and 5, and equation (7)

Reviewer 2 comment:

L129-137: If the net ecosystem exchange reduces to the sum of the eddy flux and the storage flux, then don't worry about including advection in the equation. Just state the simplifying assumptions clearly in full in the text. Note that more than just well-developed turbulence (L133-134) is needed to simplify the mass balance on the control volume (e.g., horizontal homogeneity). Please be more complete in this description in the text. Were there any concerns regarding the validity of the simplifying assumptions because of proximity of the EC system to the canopy (as mentioned previously)?

Response:

We deleted the advection terms in equation (1), and added more precision regarding the assumption of negligible advection (quality flag of stationarity and turbulence development test, (Foken et al. 2004)). Relating to a comment above we also added a preliminary analysis of the turbulence characteristics to section 2.4, which will be finalized before submitting the revised manuscript (see response to second comment). Changes: L134-140

Reviewer 2 comment:

On the calculation of the eddy flux:

- It is more accurate to state that the IRGA measures the (number) densities of CO_2 and water vapor (L142).
- Eq. 2 is not necessary with an adequate description in the text (but if you keep it define primes and the overbar). It's not the most elegant presentation in the current Eq 2…especially since the equation doesn't include the WPL terms, which are needed. Given the maturity of the EC method a text description is fine.
- L148-149. Rephrase: "Fluxes were rotated into the natural wind coordinate system using the double rotation method". Wilczak et al. isn't the best reference for the double rotation. The original is Tanner, C. B. and Thurtell, G. W.: 1969, Anemoclinometer Measurements of Reynolds Stress and Heat Transport in the Atmospheric Surface Layer, University of Wisconsin Tech. Rep., ECOM-66-G22-F, 82 pp. [Available from US Army Electronic Command, Atmospheric Sciences Laboratory, Ft. Huachuca, AZ 85613.] or referencing the chapter in the Handbook of Micrometeorology.
- L149…what time lags? Between the sonic and IRGA?
- L150-151. Block averaging is not a detrending operation.
- Check to make sure that the order of the steps in the description of the flux calculation matches what was actually done (e.g., one of the last items in the description concerns the removal of spikes in raw data, L153).

Response:

L144-166 (section 2.4)

- Concentration replaced with number density, L145
- Equation (2) deleted, the section 2.4, L144-165 describes the calculation details.
- Amended.
- Amended (yes, time lags between the sonic and IRGA, which are of course much smaller in open-path yet still recommended, due to the physical distance between the two instruments).
- Amended "We applied the block averaging method to calculate each half-hour average and fluctuation relative to the average, to calculate the covariance" L156-157
- Amended, 1. Raw data screening (spikes removal …), 2. If 10% data is missing, flux will be flagged NA 3. Rotation 4. Time lags 5. Block average 6. WPL, flux calculation 7. Flags applied, L150-165

Reviewer 2 comment:

L168-182 (section 2.5)

On the calculation of the storage flux:

- A complete description of Eq (4) is lacking (definition of all symbols etc.)
- Why were storage fluxes of water vapor not estimated? Is this a significant source of bias in LE measurements?

Response:

- Amended: added: "Where C is CO_2 (µmol m^{-3}) and t is time (s) ($\Delta C/\Delta t$ is the variation of C over 30 minutes), z is the height (m), k [1 to n = 8] represents each inlet. L175-176
- The main reason not to use the H_2O signal from the LI840 is that we do not have heated lines and the tubes will have significant adsorption/desorption issues depending on conditions. So the signal would not be reliable.
  We had a look at the 1-point estimation of H_2O storage (from the Li-7500A at 29m), and it showed a low contribution of change in H_2O storage to the total H_2O flux (see figure below). Rather than using a low quality, noisy estimate of H_2O from the 1-point estimation, we chose to assume that change in H_2O storage was negligible.

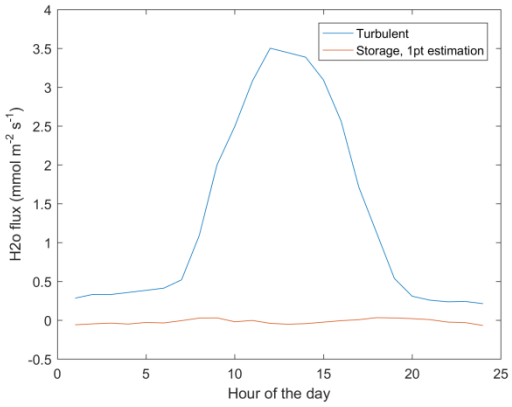

Figure 1 Diurnal course of H2o flux (mmol m^{-2} s^{-1}) turbulent exchange and change in storage (1 point estimation) in 2017.

Reviewer 2 comment:

L183. What exactly is specific heat density (SHD)?

Response:

This was a typo, SHD stands for specific humidity deficit. The section 2.6, L183-204, about gap-filling and partitioning, has been updated entirely with the most recent processing of the data, including 2017 for this revised manuscript.

Reviewer 2 comment:

L188-194. It would be worth presenting a footprint climatology in the supplementary information.

Response:

We added a footprint climatology to the supplementary information as suggested. (figure S5), referred to on L207 (section 2.7).

Reviewer 2 comment:

L195-199. Clarify whether closure was forced on the fluxes reported in the results.

Response:

We did not force closure on the fluxes reported, this was clarified in the text. L213-214.

Reviewer 2 comment:

L200-210. Why were the turbulent fluxes not substituted for available energy when calculating surface conductance? The spatial representativeness would be better.

Response:

Surface conductance was calculated using the turbulent flux of water vapor coming from evapo-transpiration and the net radiation (equation (4)). We apologise that the notation was not clear in the previous version; this has been corrected. L217-221, section 2.9

Reviewer 2 comment:

Eq 7. Check the 2nd term in the denominator on the RHS…the exponent should be -0.67. Add a citation and be sure all terms are defined.

Response:

Amended. Equation (5)

Reviewer 2 comment:

L241-244. The description of leaf-level sampling needs more detail. Since there is a reference that describes these measurements in more detail, the description in this manuscript can be abbreviated, however, a more thorough description of the basics.

- The instrument used
- More details on leaf chamber conditions…were the temps, humidity etc matched to ambient?
- Were sunlit or shaded leaves (or both) measured?
- What species were targeted?

Response:

We removed the details of the methods because we used previously published data; we provide the citation to the paper L258.

Reviewer 2 comment:

L266-267. “Summer GPP was higher (-460 ± 112 g C m-2) compared to winter GPP (-291 ± 28 g C m-2)”: -291 is higher (>) than -460. Check the manuscript for any other discrepancies when comparing magnitude and direction and ensure that the wording is correct.

Response:

Amended: Summer GPP was lower – i.e. more uptake (-400 ± 97 g C m^{-2}) compared to winter GPP (-282 ± 41 g C m^{-2}) (Table 1), that is a difference of ~ 118 g C m^{-2}. L281

Reviewer 2 comment:

L272-278. It looks like there is still hysteresis during winter (albeit less severe than in summer, Figs. 2 and 3). It might be useful to add 2 panels to Fig. 3 and show surface conductance light responses to help with underscoring the importance of stomatal regulation of C fluxes.

Response:

We agree that there is still hysteresis during winter, and we adjusted the text, L291-292. Also, we added the panels to Fig. 3 indicating light response of surface conductance as suggested by the reviewer.

Reviewer 2 comment:

L336-337. Is soil respiration in the subsoil really that important to the integral over the whole profile?

Response:

This is a good point. We have measured soil respiration in a nearby site, showing that soil respiration can be limited in summer when surface soil is dry. This is also seen in the flux data, as shown in figure 1.

Text edit: low soil moisture in the shallow layers sometimes limited decomposition (January and February 2014, January and December 2015, January, February and December 2017 see Figure 1), but often regular rainfall maintained adequate soil moisture. L352-353

Reviewer 2 comment:

L345-356. The paragraph starts out by rather definitively stating that “strong stomatal regulation” was the driver of diurnal hysteresis in NEE during summer and then becomes less clear and murkier. Seems odd to take this approach if it is was found that there was strong stomatal regulation of GPP and NEE. Revise.

Response:

The authors agreed and revised the paragraph entirely (361-376):

“A strong morning-afternoon hysteresis of NEE response to PPFD occurred in summer, and less so in winter (Figure 3). In winter, low D and moderately warm daytime air temperatures and high PPFD were sufficient to maintain high photosynthesis rates throughout most of the day (Figure 1). In summer, two possible explanations of the diurnal hysteresis of NEE are (1) ER is greater in the afternoon compared to morning or (2) GPP is lower in the afternoon compared to morning. Explanation (1) is plausible, as temperature drives autotrophic and heterotrophic respiration; however, it is unlikely to explain the hysteresis magnitude which is higher in summer compared to winter. Explanation (2) could arise from lower afternoon stomatal conductance or lower photosynthetic capacity (e.g. the maximum rate of carboxylation (Vcmax) decreases at high Ta), or a combination of both or even circadian regulation (Jones et al. 1998; Resco de Dios et al. 2015). An analysis of surface conductance showed strong stomatal regulation (Figure 2, Figure 3, Figure 5), induced by high

atmospheric demand and high air temperature (Duursma et al. 2014), limiting photosynthesis during the afternoon of warm months (see Figure S10). These diurnal patterns of NEE, GPP and ER play a strong role in regulating the seasonal carbon cycling dynamics in this ecosystem. A wavelet coherence analysis between D and GPP showed strong coherence at seasonal time scale (periods of three months), see figure S11."

Reviewer 2 comment:

L357-366. Hard to follow…especially the first sentence. Revise and clarify.

Response:

The authors agreed and revised the first sentence, L377-378:

"We observed comparable responses of leaf-level and ecosystem-level gas exchange to environmental drivers (Figure 5)."

Reviewer 2 comment:

L367. "Canopy dynamics"…be more specific about what you are referring to.

Response:
Right. We refer to leaf area index. Text amended.

Canopy dynamics → canopy dynamics (specifically, LAI in our analysis), L387

Reviewer 2 comment:

L390-393. Is the temperature/moisture regime at Cumberland Plain the only difference versus the other sites in eucalyptus forests? Are all the sites at similar ages and stages of succession?

Response:

The context of this statement is related to the climatic sensitivity of carbon fluxes and canopy conductance. While stand age or successional stage may affect the climatic sensitivity of the fluxes or conductance, all eucalyptus forests in the OzFlux network are mature and have been managed or disturbed to a similar degree (Hinko-Najera et al. 2017; Keith et al. 2012). The Cumberland Plain forest has somewhat lower LAI than the other forests, and has larger seasonal dynamics of LAI and carbon fluxes than Wombat Forest (Griebel et al. 2015). We have shown that GPP and conductance are strongly related to vapor pressure deficit (Fig 5) as well as LAI (Fig 6). Hence, a combination of stomatal conductance and leaf area are responsible for the climatic sensitivity of the site. We prefer not to expand the discussion on these points in order to maintain the focus of the paragraph, but we added a short phrase to link the statement to D, which we feel is the unique feature of our site (L409-412).

"Cumberland Plain has the highest mean annual temperature and the highest dryness index among the four Eucalyptus forest eddy-covariance sites in south-east Australia (Beringer et al. 2016), which could explain its strong sensitivity to D and hence its unique seasonality."

Reviewer 2 comment:

Figs. 2 & 3. It still looks like there is hysteresis in winter…is it that it is not statistically significant?

Response:

There is a hysteresis in winter, but of lower magnitude. The text has been corrected accordingly. L291-292

Reviewer 2 comment:

Fig. 4. Check units for apparent quantum yields (α). These values seem high.

Response:

In the figure 4 y-label, the units specify that the y-axis is multiplied by 10^{-2}, i.e. quantum yields value are around 0.02 (µmol CO_2 µmol photon^{-1}), values comparable to (Aubinet et al. 2001, fig. 10). Note that Mitscherlich equation (7) fits the slope to NEE, not to GPP (as in Michaelis-Menten), so the slope accounts for ER and is bigger.

References:

Foken, T., M. Gockede, M. Mauder, L. Mahrt, B. Amiro, and W. Munger, 2004: Post-field data quality control. *Handbook of Micrometeorology: A Guide for Surface Flux Measurement and Analysis*, **29,** 181-208.

Hinko-Najera, N., and Coauthors, 2017: Net ecosystem carbon exchange of a dry temperate eucalypt forest. *Biogeosciences*, **14,** 3781-3800.

Keith, H., E. van Gorsel, K. L. Jacobsen, and H. A. Cleugh, 2012: Dynamics of carbon exchange in a Eucalyptus forest in response to interacting disturbance factors. *Agricultural and Forest Meteorology*, **153,** 67-81.

Upside-down fluxes Down Under: CO_2 net sink in winter and net source in summer in a temperate evergreen broadleaf forest

Alexandre A. Renchon[1], Anne Griebel[1], Daniel Metzen[1], Christopher A. Williams[2], Belinda Medlyn[1], Remko A. Duursma[1], Craig VM Barton[1], Chelsea Maier[1], Matthias M. Boer[1], Peter Isaac[3], David Tissue[1], Victor Resco de Dios[4], Elise Pendall[1]

[1]*Hawkesbury Institute for the Environment, Western Sydney University, Penrith, NSW, Australia.*
[2]*Clark University, Graduate School of Geography, Worcester, Massachusetts 01610, USA.*
[3]*CSIRO Oceans & Atmosphere Flagship, Yarralumla, ACT, 2600, Australia.*
[4]*Department of Crop and Forest Sciences and Agrotecnio Center, University of Lleida, E-25198 Lleida, Spain.*

Abstract

Predicting the seasonal dynamics of ecosystem carbon fluxes is challenging in broadleaved evergreen forests because of their moderate climates and subtle changes in canopy phenology. We assessed the climatic and biotic drivers of the seasonality of net ecosystem-atmosphere CO_2 exchange (NEE) of a eucalyptus-dominated forest near Sydney, Australia, using the eddy covariance method. The climate is characterized by a mean annual precipitation of 800 mm and a mean annual temperature of 18 °C, hot summers and mild winters, with highly variable precipitation. In the ~~three~~four-year study, the ecosystem was a ~~small~~ sink ~~in 2014 (54~~each year (-225 g C m^{-2} y^{-1}~~),~~, on average, with a ~~stronger sink in 2015 (183~~standard deviation of 108 g C m^{-2} y^{-1}~~) and even stronger sink in 2016 (337 g C m^{-2} y^{-1}), but these~~); inter-annual variations were not related to ~~precipitation~~meteorological conditions. Daily net C uptake was always detected during the cooler, drier winter months (June through August), while net C loss occurred during the warmer, wetter summer months (December through February). Gross primary productivity (GPP) seasonality was low, despite longer days with higher light intensity in summer, because vapour pressure deficit (D) and air temperature (T_a) restricted surface conductance during summer while winter temperatures were still high enough to support photosynthesis. Maximum GPP during ideal environmental conditions was significantly correlated with remotely sensed enhanced vegetation index (EVI, r^2 = 0.46) and with canopy leaf area index (LAI~~) (~~, r^2 = 0.24), which increased rapidly after mid-summer rainfall events. Ecosystem respiration (ER) was highest during summer in wet soils and lowest during winter months. ER had larger seasonal amplitude compared to GPP, and therefore drove the seasonal variation of NEE. Because summer carbon uptake may become increasingly limited by ~~Atmospheric~~atmospheric demand and high temperature, and ecosystem respiration could be enhanced by rising temperature, our results suggest the potential for large-scale seasonal shifts in NEE in sclerophyll vegetation under climate change.

Keywords: net ecosystem exchange, seasonal variability, ~~Atmospheric~~atmospheric demand, canopy phenology

1. Introduction

Forests and semi-arid biomes are responsible for the majority of global carbon storage by terrestrial ecosystems (Dixon et al.,. 1994;Schimel et al., 2001; Pan et al.,. 2011; Poulter et al.,. 2014; Schimel et al. 2001). Photosynthesis and respiration by these biomes strongly influence the seasonal cycle of atmospheric CO_2 (Keeling et al., 2001;Baldocchi et al., 2016).(Baldocchi et al. 2016; Keeling et al. 2001). Continuous measurements of land-atmosphere exchanges of carbon, energy and water provide insights into the seasonality of forest ecosystem processes, which are driven by the interactions of climate, plant physiology and forest composition and structure (Xia et al.,. 2015). Net ecosystem exchange (NEE) seasonality is relatively well understood in cool-temperate ecosystems; deciduous trees can only photosynthesize when they have leaves and NEE dynamics are thus principally influenced by the phenology of canopy processes. NEE of deciduous forests thus has a more pronounced seasonality than that of evergreen conifer forests at similar latitudes (Novick et al., 2015).(Novick et al. 2015). For high-latitude evergreen conifer forests, NEE seasonality is strongly limited by cold temperature limitation of photosynthesis (Kolari et al., 2007)(Kolari et al. 2007) and respiration. In contrast, seasonality of NEE in evergreen broadleaf forests, typically occurring in warm-temperate and tropical regions, is much less well understood (Wu et al., 2016;Restrepo-Coupe et al.,. 2017; Wu et al. 2016).

The seasonality of gross primary productivity (GPP) in evergreen broadleaf forests may be driven by climate (e.g. dry/wet seasons) and/or by canopy dynamics (Wu et al., 2016).(Wu et al. 2016). In tropical evergreen forests, air temperature and day length are similar seasonally, but precipitation seasonality can be strong, with higher radiation and temperature (1 or 2 °C higher) in the dry season (Trenberth, 1983;Windsor, 1990).(Trenberth 1983; Windsor 1990). Counter-intuitively, GPP can be higher during the dry season, as cloud cover may limit productivity in the wet season (Graham et al.,. 2003; Hutyra et al. 2007; Saleska et al.,. 2003;Hutyra et al., 2007). Canopy dynamics can be an important determinant of GPP seasonality in evergreen broadleaf forests; although leaves are present in the canopy year-round in evergreen canopies, LAI may show considerable temporal variability seasonally as new leaves are produced and old leaves die, especially during leaf flush and senescence periods (Duursma et al.,. 2016; Wu et al.,. 2016). The leaf light use efficiency and water use efficiency may both vary as leaves age: young leaves and old leaves are less efficient than mature leaves, reflecting changes in photosynthetic capacity (Wilson et al.,. 2001; Wu et al.,. 2016). The timing of leaf flush and senescence can depend on the environment and on species; environmental stress, such as drought, can induce the process of senescence (Lim et al. 2007; Munné-Bosch and Alegre, 2004;Lim et al., 2007).

In temperate evergreen broadleaved forests, such as eucalypt-dominated sclerophyll vegetation in Australia, precipitation can be seasonal or aseasonal; furthermore, day length and temperature vary significantly between winter and summer. GPP can be limited by frost during winter and by drought during summer. Atmospheric demand indicated by high vapor pressure deficit (D),) and soil drought have different impacts on GPP, but they can interact to impact surface conductance (G_s) (Medlyn et al.,. 2011; Novick et al.,. 2016). In Australia's temperate eucalypt forests, canopy rejuvenation takes place in summer and is linked to heavy rainfall events (Duursma et al., 2016).(Duursma et al. 2016). However, since leaf flushing and shedding occur simultaneously in eucalypt canopies (Pook, 1984;Duursma et al., 2016)(Duursma et al. 2016; Pook 1984), the overall canopy volume can remain stable while the distribution of canopy volume changes with height (Griebel et al., 2015).(Griebel et al. 2015). Eucalypt forests in southeast Australia have been found to act as carbon sinks all year long, with greater uptake in summer (van Gorsel et al., 2013;Hinko-Najera et al.,. 2017; van Gorsel et al. 2013). Although canopy characteristics are key to understanding ecosystem fluxes, their dynamics in

Field Code Changed

Australian ecosystems can be particularly challenging to detect using standard vegetation indices ~~(Moore et al., 2016).~~(Moore et al. 2016). Nevertheless, the normalized difference vegetation index (NDVI) has successfully explained variability in photosynthetic capacity in Mediterranean, mulga and savanna ecosystems (Restrepo-Coupe et al~~.~~., 2016).

Field Code Changed

The environmental and biotic controls on the seasonal dynamics of ecosystem fluxes in broadleaved evergreen forests are still poorly understood. Our objective was to determine the seasonality of ecosystem CO_2 and H_2O fluxes in a dry sclerophyll Eucalyptus forest; we evaluated the role of environmental drivers (~~PAR~~PPFD, T_a, SWC and D) and canopy dynamics (as measured with ~~NDVI~~EVI, LAI, litter fall and leaf age) in regulating the seasonal patterns of net ecosystem exchange (NEE), gross primary productivity (GPP), ecosystem respiration (ER), evapotranspiration (ET) and surface conductance (G_s) in an evergreen forest near Sydney, Australia. We also compared leaf-level to ecosystem-level water and carbon exchange in response to drivers, in order to gain confidence in our results and gain insights about the emergent properties from leaf to ecosystem scale. We hypothesised that canopy phenology (LAI and leaf age) explains temporal variation in photosynthetic capacity (PC) and G_s. We anticipated that the ecosystem would be a carbon sink all year long.

2. Material and methods

2.1 Site description

The field site is the Cumberland Plain (AU-Cum in Fluxnet) forest SuperSite ~~(de Dios et al., 2015) of the Australian Terrestrial Ecosystem Research Network (http://www.tern.org.au/),~~(Resco de Dios et al. 2015) of the Australian Terrestrial Ecosystem Research Network (http://www.ozflux.org.au), located 50 km west of Sydney, Australia, at 19 m elevation, on a nearly flat floodplain of the Nepean-Hawkesbury River (latitude -33.61320; longitude 150.72446). Mean mid-afternoon (3 pm) temperature is 18 °C (max. 28.5 °C in January and min. 16.5 °C in July) and average precipitation is 801 mm $year^{-1}$ (mean monthly max. is 96 mm in January, and min. is 42 mm in September). The soil is classified as a Kandosol and consists of a fine sandy loam A horizon (0-8 cm) over clay to clay loam subsoil (8-40 cm), with pH of 5 to 6 and up to 5% organic C in the top 10 cm ~~(Karan et al., 2016). The flux tower is in a~~(Karan et al. 2016). The flux tower is in a mature dry sclerophyll forest, with 140 Mg C ha^{-1} aboveground biomass and stand density of ~500 trees ha^{-1}. ~~The~~The stand hosts a large population of mistletoe (*Amyema miquelii*), which decreases in abundance with increasing distance to the flux tower. The canopy structure comprises three strata, and the predominant canopy tree species are *Eucalyptus moluccana* and *E. fibrosa*~~, which grow to~~. While individual trees can exceed 25 m height, an airborne LiDAR survey from November 2015 indicates an average canopy height of ~~25~~24 m ~~and host~~within a ~~large population~~300 m radius of ~~mistletoe (*Amyema miquelii*). In addition,~~ the flux tower (supplement figure S1). The mid-canopy stratum (5-12 m) is dominated by *Melaleuca decora*~~,~~ and the understory is dominated by *Bursaria spinosa* with various shrubs, forbs, grasses and ferns present in lower abundance.

2.2 Environmental measurements

Air temperature (T_a) and relative humidity (RH) were measured using HMP45C (Vaisala, Vantaa, Finland) sensors at 7 m and 29 m heights. Vapour pressure deficit (D) was estimated from T_a and RH. ~~Photosynthetically active radiation~~Photosynthetic photon flux density above the canopy (~~PAR, W~~PPFD, µmol m^{-2} s^{-1}) was measured using an LI190SB (Licor Inc., Lincoln NE, USA), and incoming and outgoing short and longwave radiation were measured using a CNR1 radiometer (Kipp & Zonen, Delft, Netherlands). Ancillary data were logged on CR1000 or CR3000 dataloggers (Campbell Scientific, Logan UT, USA) at 30 min intervals. Mixing ratios of CO_2 in air were also measured at 0.5 m, 1 m, 2 m, 3.5 m, 7 m, 12 m, 20 m, and 29 m above the soil surface using a LI840A Gas Analyzer (Licor Inc., Lincoln NE, USA); data from each height were logged on a CR1000 datalogger once every 30 minutes (1 minute air sampling per height).

Ground heat flux and soil moisture were averaged between two locations to represent the variable shading in the tower footprint. One location had a HFP01 heat flux plate and the other ~~has~~had a self-calibrating heat flux plate (HFP01SC) (Hukseflux, XJ Delft, Netherlands) installed at 8 cm below the soil surface. The heat flux plates were paired with a CS616 water content reflectometer (Campbell Scientific, Logan UT) installed horizontally at 5 cm below the soil surface and a TCAV averaging thermocouple (Campbell Scientific, Logan UT) installed with thermocouples at 2 cm and 6 cm below the soil surface for each pair. A CS616 installed vertically measured average soil water content from 7 to 37 cm (CS616). Rainfall was measured at an open area with a tipping bucket 2 km away from the study site.

2.3 Net ecosystem exchange

Continuous land-atmosphere exchange of CO_2 mass (net ecosystem exchange, NEE) was quantified from direct measurements of the different components of the theoretical mass balance of CO_2 in a control volume:

$$NEE = F_{CT} + F_{CS} + (F_{CAH} + F_{CAV}) \quad (1)$$

Where F_{CT} is the vertical turbulent exchange flux, F_{CS} is the change in storage flux, and F_{CAH} and F_{CAV} are the horizontal and vertical advection fluxes - assumed negligible when atmospheric turbulence is sufficient (Baldocchi et al., 1988;Aubinet et al., 2012). We used change-point detection of the friction velocity (u*) threshold (Barr et al., 2013) to determine the turbulence threshold above which NEE (the sum of F_C and S_C) is independent of u*. However, we found no clear dependence of NEE on u* hence no clear threshold (Figure S1), so we used a threshold of 0.2 m s^{-1} to be conservative.

Where F_{CT} is the vertical turbulent exchange flux, and F_{CS} is the change in storage flux. Advection fluxes are assumed negligible when atmospheric turbulence is sufficient (Aubinet et al. 2012; Baldocchi et al. 1988), and when quality flags of stationarity and turbulence development test were good (Foken et al. 2004). We used change-point detection of the friction velocity (u*) threshold (Barr et al. 2013) to determine the turbulence threshold above which NEE (the sum of F_{CT} and F_{CS}) is independent of u*. However, we found no clear dependence of NEE on u* hence no clear threshold (Figure S2), so we used a threshold of 0.2 m s^{-1} to be conservative.

The calculation of each term, and the assumptions required for them to be representative of each half-hour flux are detailed below.

2.4 Vertical turbulent flux (F_{CT})

The vertical turbulent fluxes of CO_2 (F_{CT}, µmol m^{-2} s^{-1}) and water (F_{WT}, mmol m^{-2} s^{-1}) were measured using the eddy-covariance method (Baldocchi et al. 1988). Density (c) of CO_2 or water vapor (open-path IRGA (LI-7500A, Licor Inc., Lincoln NE, USA)) and vertical wind speed (w) (CSAT 3D sonic anemometer (Campbell Scientific, Logan UT, USA)) were measured at 10 Hz frequency at 29 m above the ground, and logged on a CR-3000 datalogger (Campbell Scientific, Logan UT, USA). Vertical turbulent fluxes were calculated from the 10 Hz data, using Eddy-Pro© software. Statistical tests for raw data screening followed (Vickers and Mahrt 1997), including spike count/removal, amplitude resolution, drop-outs, absolute limits and skewness and kurtosis tests. Low and high frequency spectral correction followed (Moncrieff et al. 2004), and (Moncrieff et al. 1997). The calculation allowed for up to 10% of missing 10 Hz data. (Baldocchi et al., 1988). Concentration (c) of CO_2 or water vapor (open-path IRGA (LI-7500A, Licor Inc., Lincoln NE, USA)) and vertical wind speed (w) (CSAT 3D sonic anemometer (Campbell Scientific, Logan UT, USA)) were measured at 10Hz frequency at 29 m above the ground, and logged on a CR-3000 datalogger (Campbell Scientific, Logan UT, USA). F_{CT} and F_{WT} are calculated as the average 30-minute covariance of c and w:Fluxes were rotated into the natural wind coordinate system using the double rotation method (Wilczak et al. 2001). Time lags between the sonic and IRGA were compensated using covariance maximization, within a window of plausible time lags (Fan et al. 1990). We applied the block averaging method to calculate each half-hour average and fluctuation relative to the average, to calculate the covariance (Gash and Culf 1996). Density fluctuations in the air volume were corrected using the WPL terms (Webb et al. 1980). Each half-hourly flux was associated with a quality flag (0: good quality, 1: keep for integrations, discard for empirical relationships, 2: remove from the data); these flags accounted for stationarity tests and turbulence development tests which are required for good turbulent flux measurements (Foken et al. 2004). In our 4-year record, 51% of F_{CT} fluxes had a flag of 0, 32% had a

flag of 1 and 17% had a flag of 2. Although the tower height (29m) is rather close to the average canopy height (24m), cospectra analysis showed good quality turbulent fluxes (the high frequency followed the -4/3 slope, thus we did not find any indications of systematic dampening in the cospectra, see figure S3).

~~F_{CT} or $F_{WT} = \overline{w'c'}$ (2)~~

~~Vertical turbulent fluxes were calculated from the 10 Hz data, using Eddy Pro© software. The calculation allowed for up to 10% of missing 10 Hz data. Axis rotation for tilt correction used the double rotation method (Wilczak et al., 2001). Time lags were compensated using covariance maximization, within a window of plausible time lags (Fan et al., 1990). We applied the block averaging method for de-trending (Gash and Culf, 1996). Density fluctuations in the air volume were corrected using the WPL terms (Webb et al., 1980). Statistical tests for raw data screening followed (Vickers and Mahrt, 1997), including spike count/removal, amplitude resolution, drop-outs, absolute limits and skewness and kurtosis tests. Low and high frequency spectral correction followed (Moncrieff et al., 2004), and (Moncrieff et al., 1997). Each half-hourly flux was associated with a quality flag (0: good quality, 1: keep for integrations, discard for empirical relationships, 2: remove from the data); these flags accounted for stationarity tests and turbulence development tests which are required for good turbulent flux measurements (Foken et al., 2004). In our 3-year record, 51% of F_{CT} fluxes had a flag of 0, 32% had a flag of 1 and 17% had a flag of 2.~~

2.5 Storage flux (F_{CS})

The change in storage flux (F_{CS}, µmol m^{-2} s^{-1}) was measured using a CO_2 profiler system, such that change of storage flux timestamp was the same as the turbulent flux timestamp. The change in storage flux was calculated as (Aubinet et al~~.~~, 2001):

$$F_{CS} = \frac{P_a}{R\,T_a}\int_0^h \frac{dC(z)}{dt}dz \qquad (3\underline{2})$$

Where P_a is the atmospheric pressure (P_a), T_a is the temperature (K), R is the molar gas constant, and C(z) is CO_2 (~~ppm) at the height z.~~µmol m^{-3}) at the height z. CO_2 is measured in ppm and converted to µmol m^{-3} using ideal gas law equation, where the air temperature and air pressure at each inlet is estimated from a linear interpolation between sensors at the top of the tower (29m) and sensors at the bottom of the tower (7m). As we only measure a limited number of heights, this equation becomes, in practice:

$$F_{CS} = \left(\frac{\Delta C}{\Delta t}\right)_{k=1} \times z_{k=1} + \sum_{k=2}^{n}\left\{\left[\left(\frac{\Delta C}{\Delta t}\right)_k + \left(\frac{\Delta C}{\Delta t}\right)_{k-1}\right] \times \frac{z_k - z_{k-1}}{2}\right\} \qquad (4\underline{3})$$

Where C is CO_2 (µmol m^{-3}) and t is time (s) ($\Delta C/\Delta t$ is the variation of C over 30 minutes), z is the height (m), k [1 to n = 8] represents each inlet ~~height. T_a was linearly interpolated from HMP at 29 m and 7 m~~. We flagged and replaced the storage flux with a one-point approximation during profiler outages (25% of the 3~~4~~-year record), using the change in CO_2 at 29 m height over 30 minutes as derived in EddyPro ~~(Aubinet et al., 2001)~~(Aubinet et al. 2001). These data were not used for empirical relationships, but kept for annual sum calculations. Storage flux of water vapour was assumed to be negligible. For visualisation of the diurnal course of storage flux and turbulent flux, see Figure ~~S2~~S4.

2.6 Gap-filling of environmental variables and NEE separation into gross fluxes

~~The OzFluxQC processing~~We used the PyFluxPro software~~, based on SOLO neural network, was used~~ for gap-filling climatic variables and fluxes, and for partitioning the NEE into gross primary

Field Code Changed
Formatted Table
Formatted: Justified
Formatted: Space Before: 12 pt
Formatted Table
Formatted: Space Before: 12 pt

productivity (GPP) and ecosystem respiration (ER) ~~(Hsu et al., 2002;Isaac et al., 2017), using data with~~ (Isaac et al. 2017). We only used observational data that passed the steady state and developed turbulence tests for gap-filling and for partitioning (QC flags of 0 and 1 ~~(Foken et al., 2004). In brief, gaps~~; (Foken et al. 2004)). In brief, gaps in climate variables were filled following the hierarchy of using variables provided from 1) automatic weather stations from the closest weather station, 2) numerical weather prediction model outputs (ACCESS regional, 12.5 km grid size provided by the Bureau of Meteorology) and lastly 3) monthly mean values from the site-specific climatology. In a next step the continuous climate variables were used to fill all fluxes by utilizing the embedded SOLO neural network with 25 nodes and 500 iterations on monthly windows. ~~We~~ We used 'Random Forest' (Breiman 2001) to determine and rank potential explanatory variables for explaining latent heat flux (λE), sensible heat flux (H) and NEE. We then selected the five variables with the highest feature importance for each flux and compared the gap-filling performance of the neural network for each flux with the performance based on an educated guess of potential relevant drivers ~~based on the highest r^2~~. We selected the variable array with the highest Pearson correlation coefficient (r) and lowest root mean square error (RMSE) for gap-filling in PyFluxPro, which identified net radiation (~~F_n), specific heat density (SHD~~R_n), soil water content (SWC), soil temperature (T_s), wind speed (w_s) and vapor pressure deficit (D) for λE (r = 0.93, RMSE = 32.0); down-welling shortwave radiation (F_{sd}), air temperature (T_a~~)~~), T_s, w_s , SWC and ~~wind speed (w_s)~~D for ~~latent heat flux; F_n~~H (r = 0.97, RMSE = 23.1) and F_{sd}, D, T_a ~~and w_s for sensible heat flux and D, T_a, shortwave incoming radiation (F_{sd}) for NEE. In addition~~, T_s and SWC for NEE (r = 0.87, RMSE = 4.04). To gap-fill ER, all nocturnal observational data (at night, we assume GPP = 0 so NEE = ER) that passed all quality control checks and the u*-filter were modelled using T_s, T_a and SWC as drivers~~.~~ in SOLO on the full dataset with 10 nodes and 500 iterations. Lastly, this ~~gapfilled data (~~gap-filled ER ~~from nighttime NEE)~~ was used to infer GPP as the result of NEE - ER.

2.7 Flux footprint

~~We analysed which turbulent flux was out of the footprint according to (Kljun et al., 2004), using a criterion that at least 75% of the turbulent flux (F_{C1}) should come from within the forest area. We used Nearmap high resolution aerial imagery to determine the extent of the forest ecosystem surrounding the tower. We found that, after u* filtering, CO_2 turbulent fluxes (F_{C1}) originated from the footprint of interest. We assumed that the ecosystem within the footprint was homogeneous for the purpose of this study.~~

We analysed the footprint climatology of AU-Cum site according to (Kormann and Meixner 2001), using the R-Package "FREddyPro' (Figure S5). We assumed that the ecosystem within the footprint was homogeneous for the purpose of this study.

2.8 Energy balance

We evaluated the energy balance closure with the ratio of available energy (~~net radiation (R_n)~~ – soil heat flux (G)) to the sum of turbulent heat fluxes (~~latent heat flux (L) + sensible heat flux (~~λE + H~~)~~). On a daily basis, the energy balance closure was 70% (Figure ~~S3~~S6), consistent with the well-known and common issue of a lack of closure (Foken 2008; Foken et al. 2006; Wilson et al~~.~~, 2002~~;Foken et al., 2006;Foken, 2008~~)~~.~~. We did not use the criteria that closure had to be met for the reported fluxes.

2.9 Surface conductance

~~Surface conductance (G_s) was derived by inverting the Penman-Monteith equation (Monteith, 1965):~~

Surface conductance (G_s) was derived by inverting the Penman-Monteith equation (Monteith 1965):

$$G_s = \frac{\gamma \, \lambda E \, g_a}{\Delta \, R_n + \rho \, C_p \, D \, g_a - \lambda E \, (\Delta + \gamma)} \quad (4)$$

Where γ is the temperature dependent psychrometric constant (kPa K^{-1}), λE is the latent heat flux (W m^{-2}), Δ is the temperature dependent slope of the saturation-vapor pressure curve (kPa K^{-1}), R_n is net radiation (W m^{-2}), ρ is the dry air density (kg m^{-3}), D is vapor pressure deficit (kPa), C_p is the specific heat of air (J kg^{-1} K^{-1}), and g_a is the bulk aerodynamic conductance, formulated as an empirical relation of wind speed (w_s, m s^{-1}) and friction velocity (u*, m s^{-1}) (Thom, 1972):

$$g_a = \frac{1}{\frac{U}{u^{*2}} + 6.2\,u^{*-0.67}} \frac{1}{\frac{w_s}{u^{*2}} + 6.2\,u^{*-0.67}} \quad (5)$$

In the analysis for G_s, we were interested in transpiration (T) rather than evaporation (E), so we excluded data if precipitation exceeded 1 mm in the past 2 days, 0.5 mm in the past 24 hours, and 0.2 mm in the past 12 hours (Knauer et al., 2015)(Knauer et al. 2015). We assumed that evaporation (E) is negligible using these criteria (Knauer et al., 2017)(Knauer et al. 2017), which excluded 40% of the data.

2.10 Potential evapotranspiration

Potential evapotranspiration rate (PET) was derived using Penman-Monteith equation (Monteith 1965):

$$PET = \frac{\Delta \, R_n + C_p \, \rho \, G_a \, D}{\gamma \, [\Delta + \gamma(1 + \frac{G_a}{G_{s,max}})]} \quad (6)$$

where $G_{s,max}$ is the well-watered reference surface conductance, calculated as the average of G_s at the study site when soil moisture exceeds the 75% quantile and D is above 0.9 and below 1.1 kPa (Novick et al. 2016).

2.11 Dynamics of canopy phenology (leaf area index, litter and leaf production) and photosynthetic capacity

We evaluated the dynamics of canopy leaf area index (LAI) by measuring canopy light transmittance with three under-canopy PARPPFD sensors and one above canopy PARPPFD sensor LI190SB (Licor Inc., Lincoln NE, USA) following the methods presented in (Duursma et al., 2016)(Duursma et al. 2016). Although we use the term LAI, this estimate does include non-leaf surface area (stems, branches). We collected litterfall (L_f, g m^2 $month^{-1}$) in the tower footprint approximately once per month, from nine litter traps (0.14 m^{-2} ground area) located near the understory PARPPFD sensors. We estimated specific leaf area (SLA) of Eucalyptus and mistletoe leaves by sampling approximately 50 fresh leaves of each, in June 2017 (SLA = 56.4 cm^2 g^{-1} for eucalyptus, 40.3 cm^2 g^{-1} for mistletoe). For each month, we partitioned the litter into Eucalyptus leaves, mistletoe leaves, and other (mostly woody) components. We used this SLA to estimate leaf litter production (L_p) in m^2 m^{-2} $month^{-1}$ of eucalyptus, mistletoe, and total as the sum of both. Then, we estimated leaf growth (L_g, m^2 $month^{-2}$) as the sum of the net change in LAI (ΔL) and L_p. Photosynthetic capacity (PC) is defined as median GPP when PARPPFD is 800-1200 Wμmol m^{-2} s^{-1} and D is 1.0 to 1.5 kPa.

Formatted Table
Formatted: Space Before: 12 pt
Field Code Changed
Formatted Table
Formatted: Space Before: 12 pt
Formatted Table
Formatted: Space Before: 12 pt
Formatted: Subscript

2.12 Analysis of light-response of NEE

We evaluated the light response of NEE using a saturating exponential function (Eq. 5) to test whether parameters varied between seasons (~~Mitscherlich, 1909;~~Aubinet et al~~.~~., 2001; Lindroth et al~~.~~., 2008; Mitscherlich 1909).

$$NEE = -(NEE_{sat} + R_d)\left(1 - \exp\left[\frac{-\alpha\, PAR}{NEE_{sat} + R_d}\right]\right)(NEE_{sat} + R_d)\left(1 - \exp\left[\frac{-\alpha\, PPFD}{NEE_{sat} + R_d}\right]\right) + R_d \quad (5)$$

where the parameter R_d is the intercept, or NEE in the absence of light, often called dark respiration; NEE_{sat} is NEE at light saturation and α is the initial slope of the curve, expressed in µmol CO_2 µmol photon^{-1} and representing light use efficiency when ~~photosynthetically active radiation (PAR~~photosynthetic photon flux density (PPFD) is close to 0. We only used daytime quality checked NEE data to fit the model (qc = 0; ~~(Foken et al., 2004)~~(Foken et al. 2004), LI-7500 signal strength = max, all inlets of profiler system data available and u* > 0.2 m s^{-1}), see Figure ~~S4~~S7.

2.13 Leaf gas exchange spot measurements

~~Spot measurement of leaf-level net photosynthesis at light saturation A_{max} (PAR ~ 1800 W m^{-2}), transpiration T, stomatal conductance g_s, and D were measured at 1.5 km for the flux tower site, see (Gimeno et al., 2016).~~

Formatted Table

Formatted: Space Before: 12 pt

We used previously published data of spot leaf gas exchange measurements in a nearby site for comparison with ecosystem fluxes (Gimeno et al. 2016).

3. Results

3.1 Seasonality of environmental drivers and leaf area index

Climatic conditions were favorable for growth at the site year-round. The monthly average of daily maximum ~~of~~ air temperature was 16.3 °C during the coldest month (July 2015), and the lowest monthly average of daily maximum ~~PAR~~PPFD was 878 µmol m^{-2} s^{-1} in the winter (June 2015; Figure 1c). Although less rainfall occurred during winter months compared to summer months, precipitation occurred throughout the year (Figure 1b). Soil volumetric water content in the shallow (0-8 cm) layer was about 10% except immediately following rain events (Figure 1b). In contrast, soil water content in the clay layer (8 -38cm) remained above 30% for the duration of the study (data not shown). ~~Average~~Monthly average of daily maximum ~~of~~ air temperature ranged from 16.3 °C in July 2015 to ~~31~~32.7 °C in ~~December 2016; Average~~January 2017; monthly average of daily maximum D ranged from 0.9 kPa in June 2015 to 3.4 kPa in ~~December 2016~~January 2017 (Figure 1c). For visualisation of seasonal and diurnal ~~trend~~trends of radiation, air temperature, D and SWC, see supplement Figure ~~S5~~S8.

Canopy leaf area index varied between 0.7 (in December 2014) and 1.1 m^2 m^{-2} (in February 2015) (Figure 1d). LAI followed a distinct pattern: it peaked in late summer (around January), and then continuously decreased until the new leaves emerged the following year. A late leaf flush was observed in 2017 (April). Litter production was concurrent with leaf growth and also peaked in summer, before and during the leaf flush, and was lower in winter (Figure 1d).

3.2 Seasonality of carbon and water fluxes

Contrary to expectations, the ecosystem was always a sink for carbon in winter (~~-127~~146 g C m^{-2} ~~in 2014, -135~~on average, with a standard deviation of 22 g C m^{-2} ~~in 2015 and -99 g C m^{-2} in 2016~~), and usually a carbon source or close to neutral in summer (+~~97~~ 44 g C m^{-2} ~~in 2014, +31~~on average, with a standard deviation of 43 g C m^{-2} ~~in 2015 and -15 g C m^{-2} in 2016~~) (Table 1). On average, summer ~~Summer~~ GPP was ~~higher (-460 ± 112~~lower – i.e. more uptake (-400 ± 97 g C m^{-2}) compared to winter GPP (~~-291 ± 28~~282 ± 41 g C m^{-2}) (Table 1), that is a difference of ~ ~~169~~118 g C m^{-2}. However, average summer ER was much higher (~~497 ± 57~~444 ± 56 g C m^{-2}) compared to winter ER (~~171 ± 26~~159 ± 35 g C m^{-2}) (Table 1), a difference of ~ ~~326~~285 g C m^{-2}. The summer vs. winter ER difference was ~~close to~~more than double the GPP difference; thus, ER had a relatively larger effect over the seasonality of NEE.

Formatted: Font: 10 pt

3.3 Diurnal trend of CO_2 flux and drivers in winter and summer

The diurnal pattern of NEE in clear-sky conditions differed between summer and winter (Figure 2). Relatively speaking, diurnal NEE was more symmetric in the winter than in summer. That is, morning and afternoon NEE pattern resembled a mirror image and total integrated morning NEE was similar to integrated afternoon NEE during the winter, but strong hysteresis occurred in the summer (Figure 2). This pattern also translated into hysteresis in the NEE light response curve in summer, but ~~not~~to a lesser degree in winter (Figure 3).

3.4 Analysis of NEE light response curve

The parameters of the NEE light response in summer and winter are shown in Figure 4 (see methods, Eq. 5). The initial slope of NEE with light (α) showed no clear dependence on T_{soil} in winter but exhibited sensitivity during summer, dropping precipitously at soil temperature above 23 °C (Figure 4a). α increased with SWC in winter and summer by a factor of ~~2~~1.5 (Figure 4b). In both winter and summer α decreased with D (D > 1 kPa) and in a similar fashion, approaching ~~to~~ a saturating value of 0.01 (µmol $µmol^{-1}$) at a D of about 2 kPa (Figure 4c). The fitted NEE at saturating light (NEE_{sat}) was

not related to T_{soil} in winter but decreased with increasing T_{soil} in summer (Figure 4d). NEE_{sat} was higher in winter than in summer for a given SWC. The relationship with D was more complicated, tending to increase with D in winter, but decreasing with increased D in summer, dropping from 9 to 3 (µmol m^{-2} s^{-1}) as D increased from 1 to 4 kPa. R_d was significantly higher in summer than winter across all conditions of T_{soil}, SWC and D (Figure 4g, h, i). R_d increased with T_{soil} in winter and less so in summer. In winter, R_d increased ~~with SWC in dry condition in winter and plateaued at~~ up to SWC of 11%; in summer, R_d was more sensitive to SWC ~~in summer~~, doubling from a rate of ~ 4 ~~in dry soils~~ to ~ 8 µmol m^{-2} s^{-1} ~~in wet soils.~~as SWC increased from about 8 to 20%.

3.5 Atmospheric demand and soil drought control on GPP, ET, G_s and WUE

We evaluated the effect of soil water content (SWC at 0-8 cm depth) and vapour pressure deficit (D) on GPP, ET, water use efficiency (WUE) and canopy conductance (G_s) under high radiation ("~~PAR-saturared"; PAR~~light-saturated"; PPFD > 1000 ~~W~~µmol m^{-2} s^{-1}), after filtering periods following rain events in order to minimise the contribution of evaporation to ET (see Methods) (Figure 5). In summer, ~~PAR~~light-saturated GPP decreased above D ~ 1.3 kPa, but in winter, GPP did not vary with D. In summer and in winter, GPP increased with SWC (Figure 5a). This is consistent with Figure 4, where R_d and NEE_{sat} both increased with SWC. In summer, ~~PAR~~light-saturated ET increased with D up to ~1.3 kPa, above which it reached a plateau. In winter, ET kept increasing with D, as D rarely exceeded 2 kPa. In both seasons, ET increased with SWC (Figure 5b). Surface conductance decreased with D and SWC especially in summer, indicating strong stomatal regulation (Figure 5~~b~~d). Water use efficiency (WUE) decreased with increasing D in summer and in winter, because ET increased but GPP declined (Figure 5c).

We compared these ecosystem-scale results to the equivalent at the leaf-scale, which are net photosynthesis at light saturation A_{max} (~~PAR~~PPFD ~ 1800 ~~W~~µmol m^{-2} s^{-1}), leaf transpiration T, leaf water use efficiency, and stomatal conductance g_s. (Figure 5, black lines). These leaf level measurements are expressed on a leaf-area basis, as ~~opposite~~compared to ground area for ecosystem scale. We observed that A_{max}, T and g_s were more sensitive to D than corresponding ecosystem-scale responses. A_{max} was much higher than GPP_{max} at D ~ 1 kPa, while g_s was comparable in magnitude to G_s in the same condition. Leaf transpiration peaked around D = 1.2 kPa, while ET plateaued. Leaf water use efficiency was overall higher than ecosystem WUE.

3.6 Canopy phenology control ~~on~~of GPP

Monthly average ~~of~~ photosynthetic capacity (PC) varied by a factor of ~2.~~7~~ across the study period, ranging from ~~6~~8.4 µmol m^{-2} s^{-1} before the leaf flush in November ~~2015~~2014 to ~~19.4~~15 µmol m^{-2} s^{-1} after the leaf flush occurred in March 2016. We expected that PC could be predicted by LAI ~~and/or NDVI~~, EVI and G_s. Leaf area index (LAI) and photosynthetic capacity (PC) were significantly correlated; the slope was significantly different from zero (r^2 = 0.24, p ~~=~~< 0.~~02~~005, PC = ~~10.9~~8.8 LAI + ~~1.8~~3.7, Figure 6). ~~By contrast, NDVI~~ EVI was ~~not~~even more significantly correlated with PC (~~(r^2 =~~ 0.46, p < 0.005, PC = 52 EVI – 5.3, Figure 6). $G_{s,max}$ was significantly correlated with PC (~~p = 0.05,~~ r^2 = 0.~~14~~2, p < 0.005, PC = ~~52~~09 $G_{s,max}$ + ~~8.6~~9) and LAI (~~p = 0.006,~~ r^2 = 0.~~25~~27, p < 0.005, $G_{s,max}$ = 0.~~01~~51 LAI ~~– 1.8e-3~~ – 0.17) and with ~~NDVI (p = 0.003,~~ EVI (r^2 = 0.~~24~~29, p < 0.005, $G_{s,max}$ = 2.3 EVI – 0.~~015 NDVI – 4.4e-3).~~45). The correlations with NDVI were less significant than with EVI (see figure S9).

398

14

4. Discussion

We measured ~~three~~four consecutive years of carbon, water and energy fluxes in a native evergreen broadleaf Eucalyptus forest, including canopy dynamics and environmental drivers (photosynthetically active radiation, air and soil temperature, precipitation, soil water content, and atmospheric demand). We hypothesised that the Cumberland Plain forest would be a carbon sink all year-round, similar to other eucalypt forests (~~Keith et al., 2012;~~Beringer et al~~.~~, 2016; Hinko-Najera et al~~.~~, 2017; Keith et al. 2012). We also hypothesised higher net carbon uptake during summer, due to warmer temperatures, higher light and longer day length contributing to higher photosynthesis, compared to winter. However, the ~~Cumberland Plain forest~~site was a net source of carbon during summer, and a net sink of carbon during winter.

The seasonal pattern of NEE was driven mostly by ER, as the seasonal amplitude of ER was larger than the seasonal amplitude of GPP. The seasonality of ER may be explained by the positive effects of higher temperatures on the rates of autotrophic respiration ~~(Tjoelker et al., 2001)~~(Tjoelker et al. 2001), and on the activity of microbes to increase soil organic matter decomposition ~~(Lloyd and Taylor, 1994)~~(Lloyd and Taylor 1994); low soil moisture ~~remained high enough to rarely limit~~in the shallow layers sometimes limited decomposition~~, especially in the subsoil.~~ (January and February 2014, January and December 2015, February and December 2017, see Figure 1), but often regular rainfall maintained adequate soil moisture. The relatively low seasonality of GPP may be partly explained by lower photosynthetic capacity in early summer (before January) when LAI ~~is~~was at its lowest, and the leaves have reached maximum age because new leaves have not yet emerged. The ER-driven seasonality of NEE is in sharp contrast with cold temperate forests where GPP drives the seasonality of NEE. ER-driven NEE seasonality was also observed in an Asian tropical rain forest, as ER was higher than GPP in the rainy season leading to net ecosystem carbon loss, while in the dry season, ecosystem carbon uptake was positive ~~(Zhang et al., 2010)~~(Zhang et al. 2010). This pattern was also observed in an Amazon tropical forest (Saleska et al~~.~~, 2003).

Field Code Changed

~~Diurnal~~ A strong morning-afternoon hysteresis of NEE response to PPFD occurred in summer ~~was associated with strong stomatal regulation, induced by high atmospheric demand and high air temperature (Duursma et al., 2014), limiting photosynthesis during the afternoon of warm months (see Figure S6).~~, and less so in winter (Figure 3). In winter, low D and moderately warm daytime air temperatures and high ~~PAR~~PPFD were sufficient to maintain high photosynthesis rates throughout most of the day~~. Two~~ (Figure 1). In summer, two possible explanations of the diurnal hysteresis of NEE ~~in summer~~ are (1) ER is greater in the afternoon compared to morning or (2) GPP is lower in the afternoon compared to morning. Explanation (1) is plausible, as temperature drives autotrophic and heterotrophic respiration; however, it is unlikely ~~as~~to explain the hysteresis ~~only happened~~magnitude which is higher in summer~~, and not in~~ compared to winter. Explanation (2) could arise from lower afternoon stomatal conductance or lower photosynthetic capacity~~,~~ (e.g. the maximum rate of carboxylation (Vcmax) decreases at high T_a), or a combination of both or even circadian regulation ~~(de Dios et al., 2015;Jones et al., 1998).~~(Jones et al. 1998; Resco de Dios et al. 2015). An analysis of surface conductance showed strong stomatal regulation (Figure 2, Figure 3, Figure 5), induced by high atmospheric demand and high air temperature (Duursma et al. 2014), limiting photosynthesis during the afternoon of warm months (see Figure S10). These diurnal patterns of NEE, GPP and ER play a strong role in regulating the seasonal carbon cycling dynamics in this ecosystem. A wavelet coherence analysis between D and GPP showed strong coherence at seasonal time scale (periods of three months), see figure S11.

We observed comparable ~~light saturated leaf|ecosystem A_{max}|GPP, T|ET, WUE and g_s|G_s~~ responses ~~to D~~ (of leaf-level and ecosystem-level gas exchange to environmental drivers (Figure 5). The ~~difference in~~larger magnitude of ~~GPP and~~ A_{max} than GPP at high D may be explained by the proportion of shaded leaves~~: LAI is around 1 m^2 [leaf area] m^{-2} [ground area], a proportion of these leaves are in the shadow, it is thus expected that A_{max} (expressed per m^2 of leaves) will be higher~~ in the ecosystem. The similar magnitude for G_s and g_s was also expected, as LAI is close to 1 and R_n is not a driver for stomatal conductance. The peaked pattern of T versus D, as opposite to ~~plateaued~~saturating pattern of ET, may be explained by (1) the contribution of soil evaporation to ET or (2) the presence of mistletoe, known for not regulating their stomata ~~(Griebel et al., 2017).~~(Griebel et al. 2017). The higher magnitude of leaf water use efficiency results from the combination of higher A_{max} and similar or lower leaf transpiration compared to ET. Furthermore, we compared leaf level g_1 and ecosystem level G_1, using the optimal stomatal conductance model (Medlyn et al. 2011): G_1 was lower than g_1 (1.6 ± 0.06 for G_1, 4.4 ± 0.2 for g_1, see figure S12).

Our study demonstrated that canopy dynamics (specifically, LAI in our study) play an important role in regulating seasonal variations in GPP even in evergreen forests. Similar observations emerged from a tropical forest, where leaf area index and leaf age explained the seasonal variability of GPP (Wilson et al~~.~~, 2001; Wu et al~~.~~, 2016), as the photosynthetic capacity (PC, the maximum rate of GPP in optimal environmental condition) varied with leaf age. In Australian woodlands, PC (A_{max}) of leaves was also found to decrease with leaf age, A_{max} declined by 30% on average between young and old leaves, for 10 different species (Reich et al. 2009). In the Cumberland Plain forest, periods with high LAI co-occur with mature, efficient leaves, and periods with low LAI co-occur with old, less efficient leaves. LAI was correlated with PC, which was probably the result of both a greater number of leaves and more efficient leaves. Remotely sensed vegetation indices such as ~~enhanced vegetation index (EVI) or normalized difference vegetation index~~(EVI) or (NDVI) assess whether the target being observed contains live green vegetation. In Australia, NDVI and EVI were good predictors of photosynthetic capacity in savanna, mulga and Mediterranean-mallee ecosystems ~~(Restrepo-Coupe et al., 2016). However, for Cumberland Plain forest NDVI was a poor predictor of PC, which could be explained because (1) greenness did not drive photosynthetic potential, which could be because the understory greening has only subtle influence on PC or (2) there is a bias or a scale mismatch in the NDVI measurements. Unfortunately, satellite-derived LAI values are~~(Restrepo-Coupe et al. 2016). For our site, EVI was a good predictor of PC, which was surprising as satellite-derived LAI values have been found to be typically inaccurate in open forests and forests in southeast Australia ~~(Hill et al., 2006), which might also indicate limitations of satellite products to establish successful relations between NDVI and GPP in sclerophyll ecosystems.~~(Hill et al. 2006). NDVI was a poor predictor of PC (see figure S9).

In a global study, it was shown that mean annual NEE decreased with increasing dryness index (PET/P) in sites located below 45° N latitude ~~(Yi et al., 2010).~~(Yi et al. 2010). It has also been shown that *Eucalyptus* grow more slowly in warm environments ~~(Prior and Bowman, 2014). At Cumberland Plain, and in a previous study~~(Prior and Bowman 2014). At our site, and in a previous study in Eucalyptus forest ~~(van Gorsel et al., 2013)~~(van Gorsel et al. 2013), GPP decreased with D above a threshold of ~ 1.3 kPa. Our results indicate that surface conductance (G_s) decreased above that threshold, suggesting that the decrease in GPP is caused by stomatal regulation. As D correlates with air temperature, it is difficult to distinguish the relative contribution of D and T_a to the decrease of G_s, but they are thought to both impact G_s ~~(Duursma et al., 2014). The~~(Duursma et al. 2014). Cumberland Plain has the highest mean annual temperature and the highest dryness index among the four

Eucalyptus forest eddy-covariance sites in south-east Australia (Beringer et al. 2016), which could explain its strong sensitivity to D and hence its unique seasonality.

5. Conclusions

The Cumberland Plain forest was a net C source in summer and a net C sink in winter, in contrast to other Australian eucalypt forests which were net C sinks year-round. ER drove NEE seasonality, as the seasonal amplitude of ER was greater than GPP. ER was high in the warmer, wetter months of summer, when environmental conditions supported high autotrophic respiration and heterotrophic decomposition. Meanwhile, GPP was limited by lower LAI and probably older leaves in early summer, and by high D which limited G_s throughout the summer. Despite being evergreen, there was significant temporal variation in LAI, which was correlated with monthly photosynthetic capacity~~.~~ and monthly surface conductance. Understanding LAI dynamics and its response to precipitation regimes will play a key-role in climate change feedback.

Code and data availability

All the datasets and scripts used in this manuscript can be downloaded at: ~~https~~http://doi.org/10.5281/zenodo.~~1069862~~1219977

Author contribution

DT, VRD, EP, AAR conceived the project; CVMB, CM, EP, AAR, AG, MMB, DM collected the data and assured the maintenance of the experiment; AAR, AG, DM, CAW, EP, PI, VRD, analysed the data; AAR, EP, ~~VDR~~VRD wrote the manuscript with input from all other authors.

The authors declare that they have no conflict of interest.

Acknowledgements

The Australian Education Investment Fund, Australian Terrestrial Ecosystem Research Network, and Hawkesbury Institute for the Environment at Western Sydney University supported this work. We thank Jason Beringer, Helen Cleugh, Ray Leuning~~, Dan Metzen~~ and Eva van Gorsel for advice and support. Senani Karunaratne provided soil classification details.

514

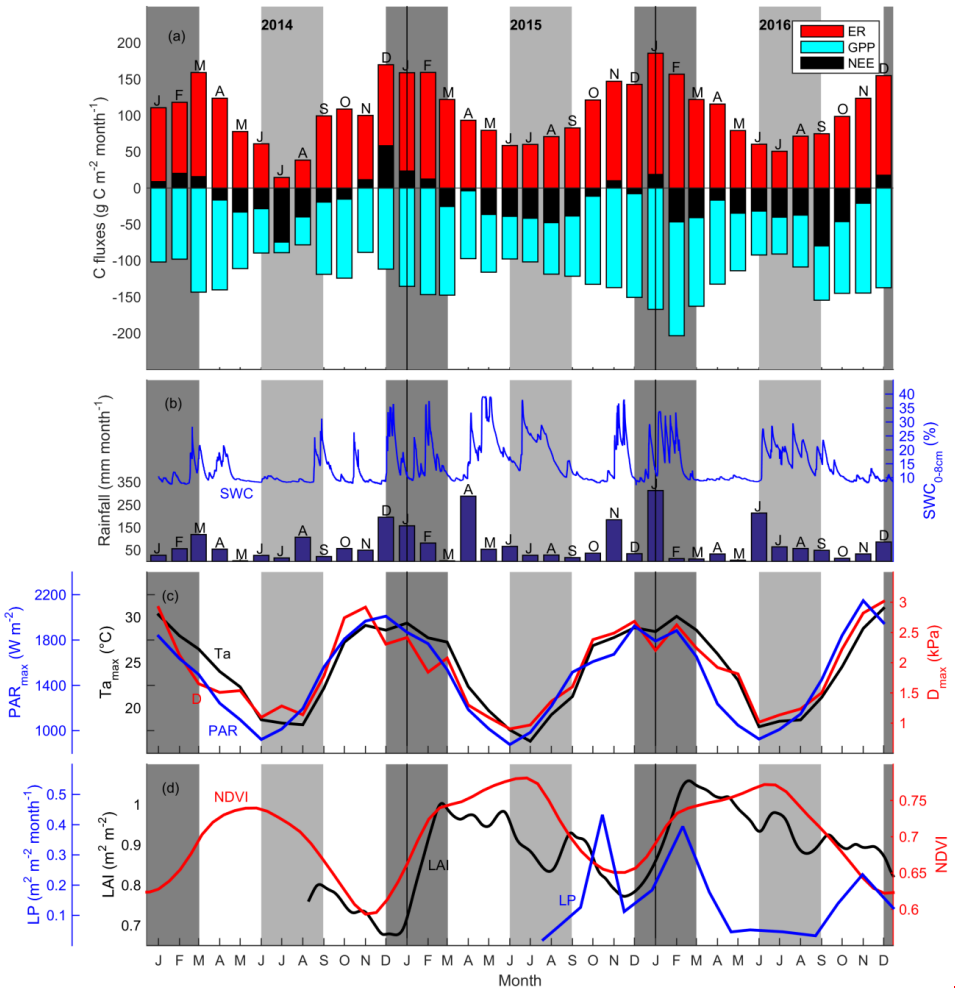
(a)
2014
2015
2016
ER
GPP
NEE
C fluxes (g C m-2 month-1)
(b)
Rainfall (mm month-1)
SWC
SWC0-8cm (%)
(c)
PARmax (W m-2)
Tamax (°C)
Ta
D
PAR
Dmax (kPa)
(d)
LP (m2 m-2 month-1)
LAI (m2 m-2)
NDVI
LAI
LP
Month

515

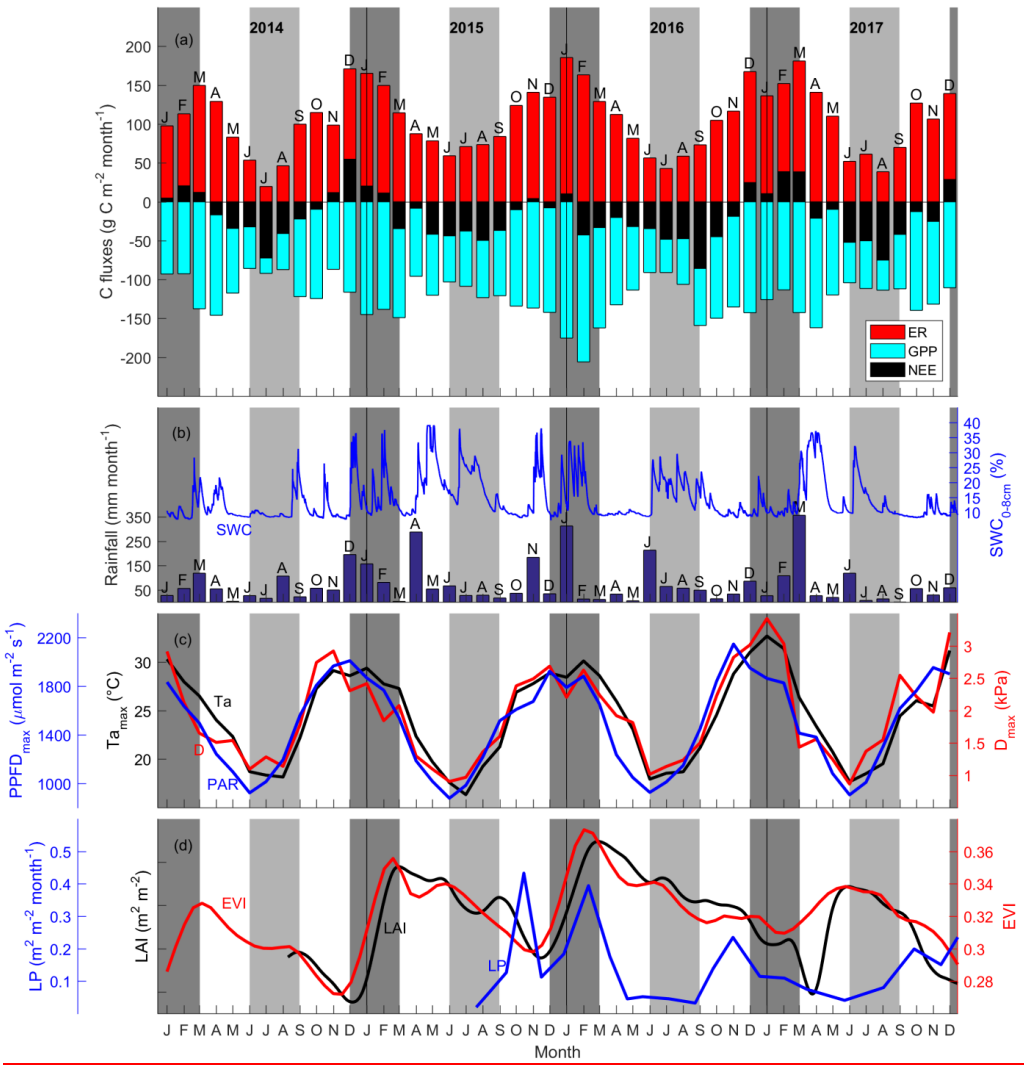

Figure 1 a) Time series of monthly carbon flux (net ecosystem exchange (NEE), ecosystem respiration (ER) and gross primary productivity (GPP), g C m^{-2} $month^{-1}$) (negative indicates ecosystem uptake); b) rainfall, mm $month^{-1}$; soil water content from 0 to 8 cm (~~SWC 0~~SWC_{0-8cm}, %); c) average of daily maximum for each month photosynthetically active radiation (~~PARmax, W~~$PPFD_{max}$, µmol m^{-2} s^{-1}), air temperature (Ta_{max} , °C) and vapour pressure deficit (D_{max}, kPa~~)~~). d) Canopy dynamics trends ~~[normalized difference~~; enhanced vegetation index (~~NDVI~~EVI, unitless); ~~d)~~ leaf area index (LAI, m^2 m^{-2}) ~~from November 2013 to April 2016~~ and litter production (L_P, m^2 m^{-2} $month^{-1}$~~)~~.). Shaded areas shows summer (dark grey) and winter (light grey). Note Ta_{max} and ~~PAR~~$_{max}$$PPFD_{max}$ remained above 15 °C and 800 ~~W~~µmol m^{-2} s^{-1}.

Formatted: Subscript

Formatted: Subscript

524

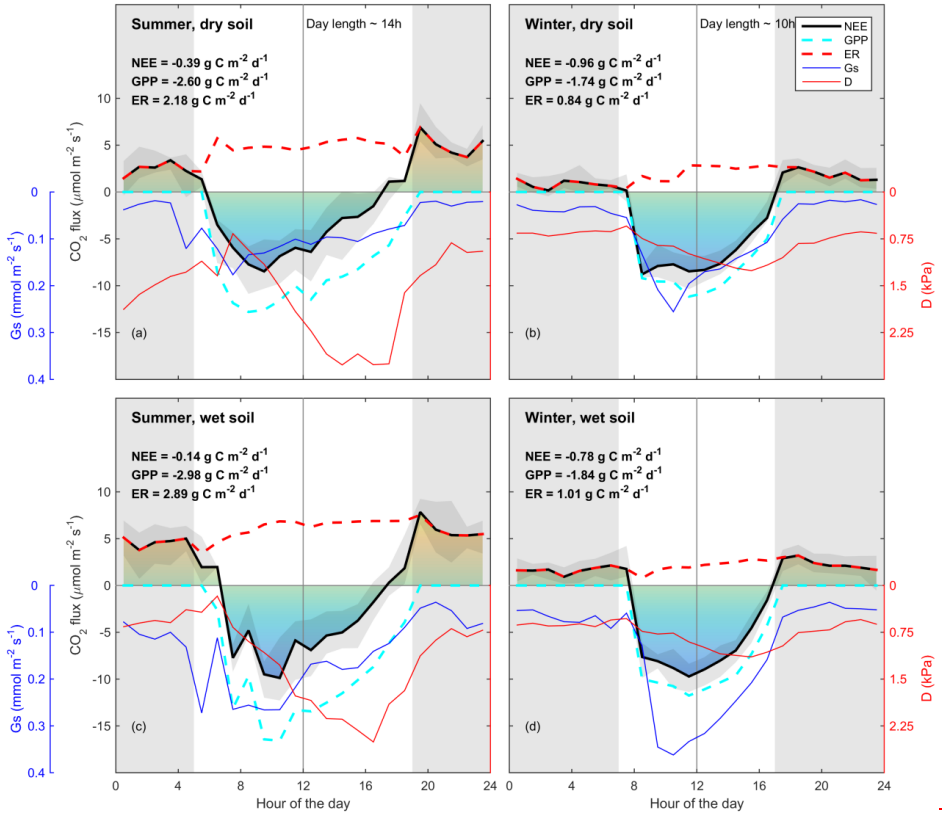
Summer, dry soil
Day length ~ 14h
NEE = -0.39 g C m-2 d-1
GPP = -2.60 g C m-2 d-1
ER = 2.18 g C m-2 d-1
(a)
Winter, dry soil
Day length ~ 10h
NEE = -0.96 g C m-2 d-1
GPP = -1.74 g C m-2 d-1
ER = 0.84 g C m-2 d-1
(b)
NEE
GPP
ER
Gs
D
Summer, wet soil
NEE = -0.14 g C m-2 d-1
GPP = -2.98 g C m-2 d-1
ER = 2.89 g C m-2 d-1
(c)
Winter, wet soil
NEE = -0.78 g C m-2 d-1
GPP = -1.84 g C m-2 d-1
ER = 1.01 g C m-2 d-1
(d)
CO2 flux (μmol m-2 s-1)
Gs (mmol m-2 s-1)
D (kPa)
Hour of the day

525

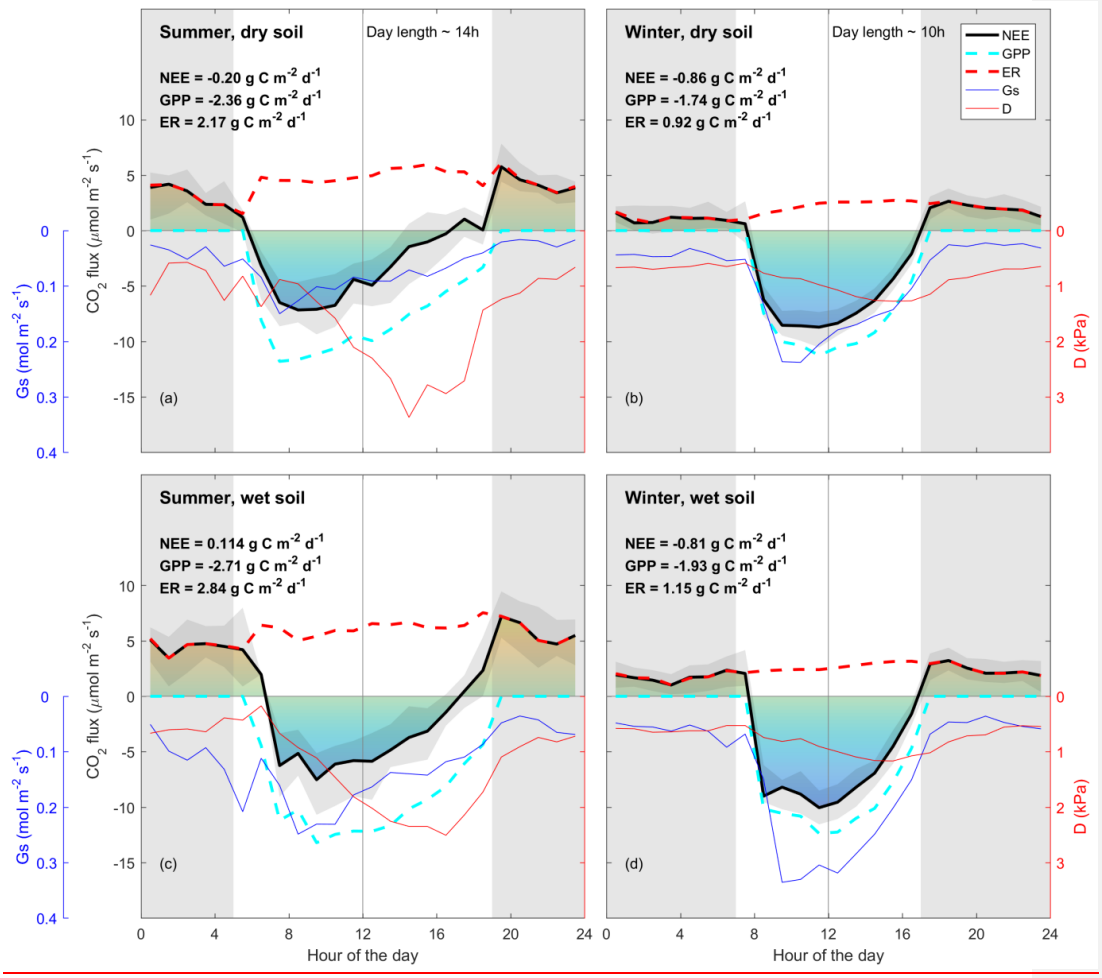

Figure 2 Diurnal trend (line: median and shade: quartile) of clear-sky measured net ecosystem exchange (NEE, thick black line, μmol m^{-2} s^{-1}); estimated daytime ecosystem respiration (ER, inferred from a neural network fitted on nighttime NEE, thick dotted red line, μmol m^{-2} s^{-1}); estimated gross primary productivity (GPP, inferred as NEE – estimated daytime ER, thick dotted cyan line, μmol m^{-2} s^{-1}); measured vapour pressure deficit (D, thin red line, kPa); and estimated surface conductance (G_s, inferred from Penman-Monteith, blue line, mmol m^{-2} s^{-1}). Grey shade shows night-time (sunset to sunrise). NEE, GPP and ER number are calculated by integrating the diurnal fluxes as shown in the figure. "Wet" and "dry" soil is defined as below or above the median of soil water content during summer or winter. Summer is December through February. Winter is June through August, as defined by the Sydney bureau of meteorology. Colours under NEE rate are shown for visualisation. Note that there is an asymmetry between morning and afternoon NEE in summer, ~~but not~~less so in winter. Note that ecosystem respiration (nighttime NEE) is enhanced by SWC in summer, ~~but not~~less so in winter. Data used in this figure correspond to clear-sky half-hour values, where high quality measured data for NEE were available.

538

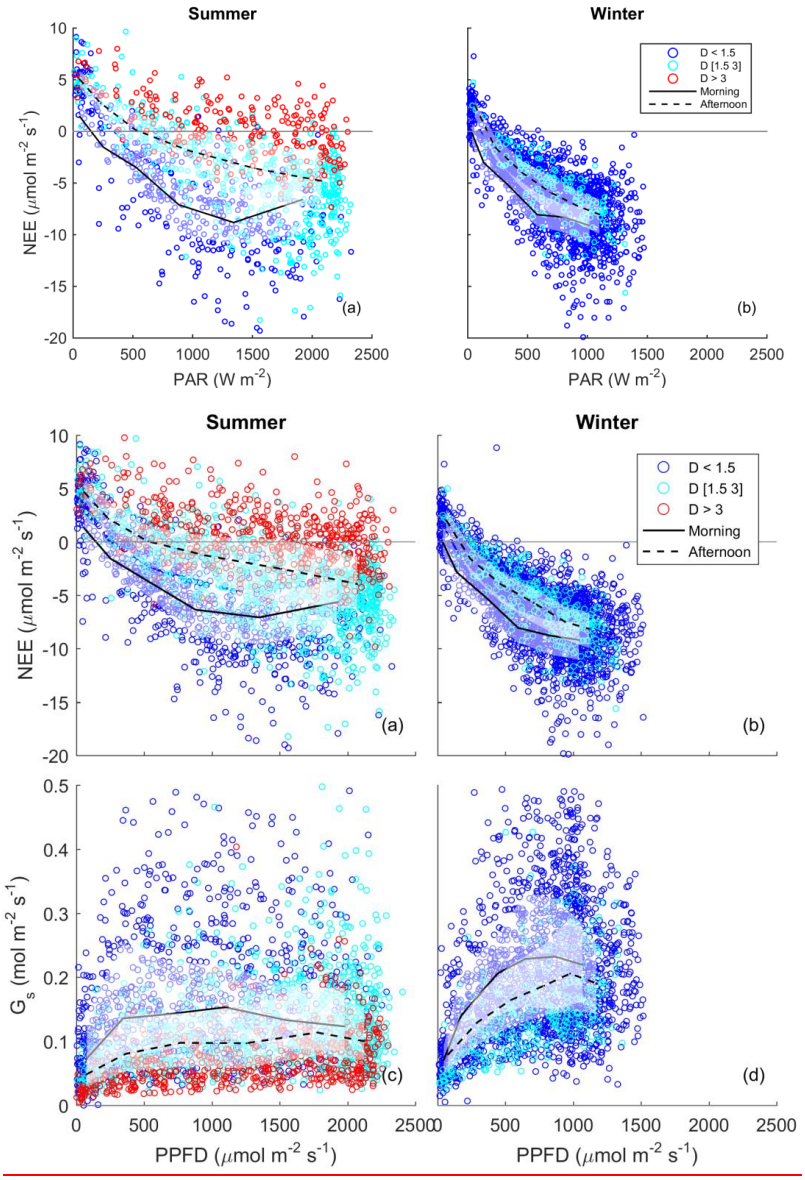

539

540

541 **Figure 3** Half-hourly measured NEE vs. ~~PAR~~PPFD, coloured by D (blue, D < 1.5 kPa, cyan: D [1.5-3] kPa, red: D > 3 kPa)
542 for (a) summer, and (b) winter periods. Raw data are binned by light levels to show median (lines) and quartiles (white
543 shades) for morning (continuous lines) and afternoon (dotted lines) hours separately.

544

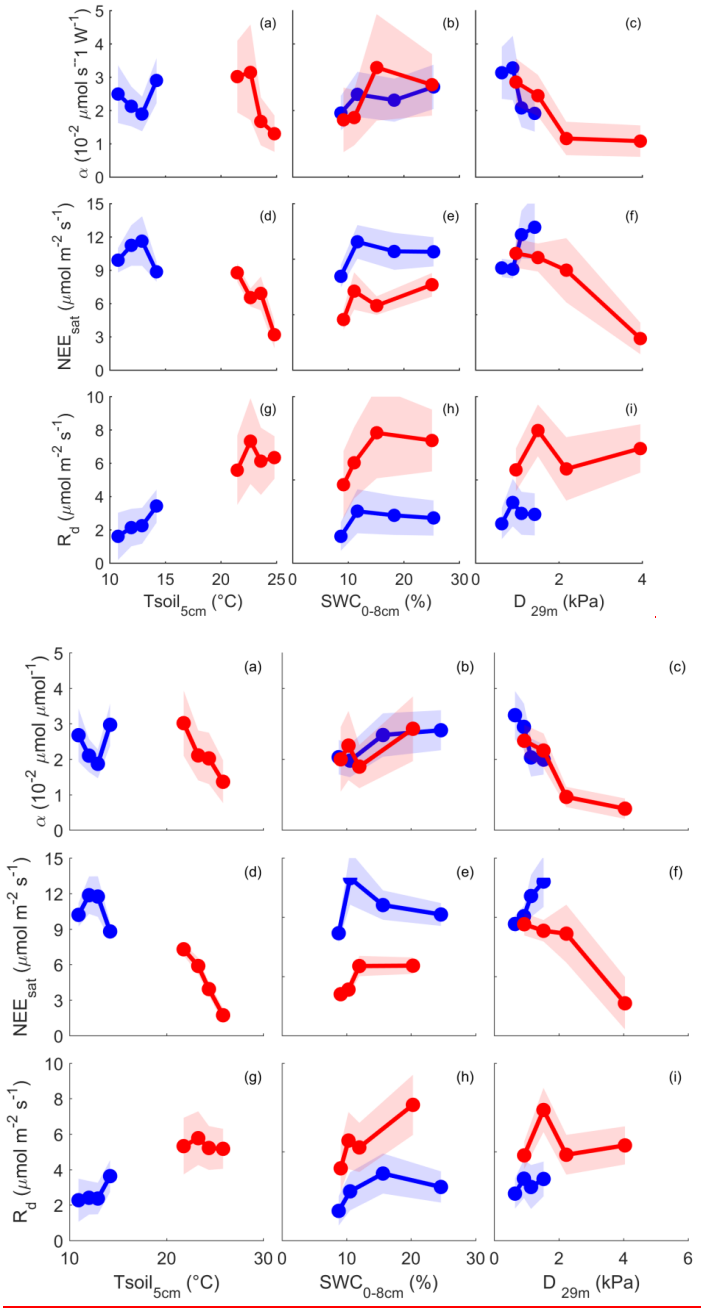

Figure 4 NEE µmol m^{-2} s^{-1} light response parameters, calculated for different bins of climatic drivers (soil temperature (T_{soil}, °C) at 5cm depth, soil water content (SWC, %) from 0 cm to 8 cm depth, and atmospheric demand (D, kPa) at ~~30~~29 m height), only raw, qc filtered daytime data is used. Light response curve was fitted using Mitscherlich equation (see methods), α is the initial slope, near ~~PAR~~PPFD = 0 (µmol ~~s^{-1} W~~µmol^{-1}), NEE_{sat} µmol m^{-2} s^{-1} is NEE at light saturation, and R_d µmol m^{-2} s^{-1} is the dark respiration (NEE when ~~PAR~~PPFD = 0). Blue indicates winter months, Red indicates summer months. Dots are parameters value for each quartile of driver, plotted at x = median of driver for each bin. Shading is 95% confidence interval of the parameter fit.

554

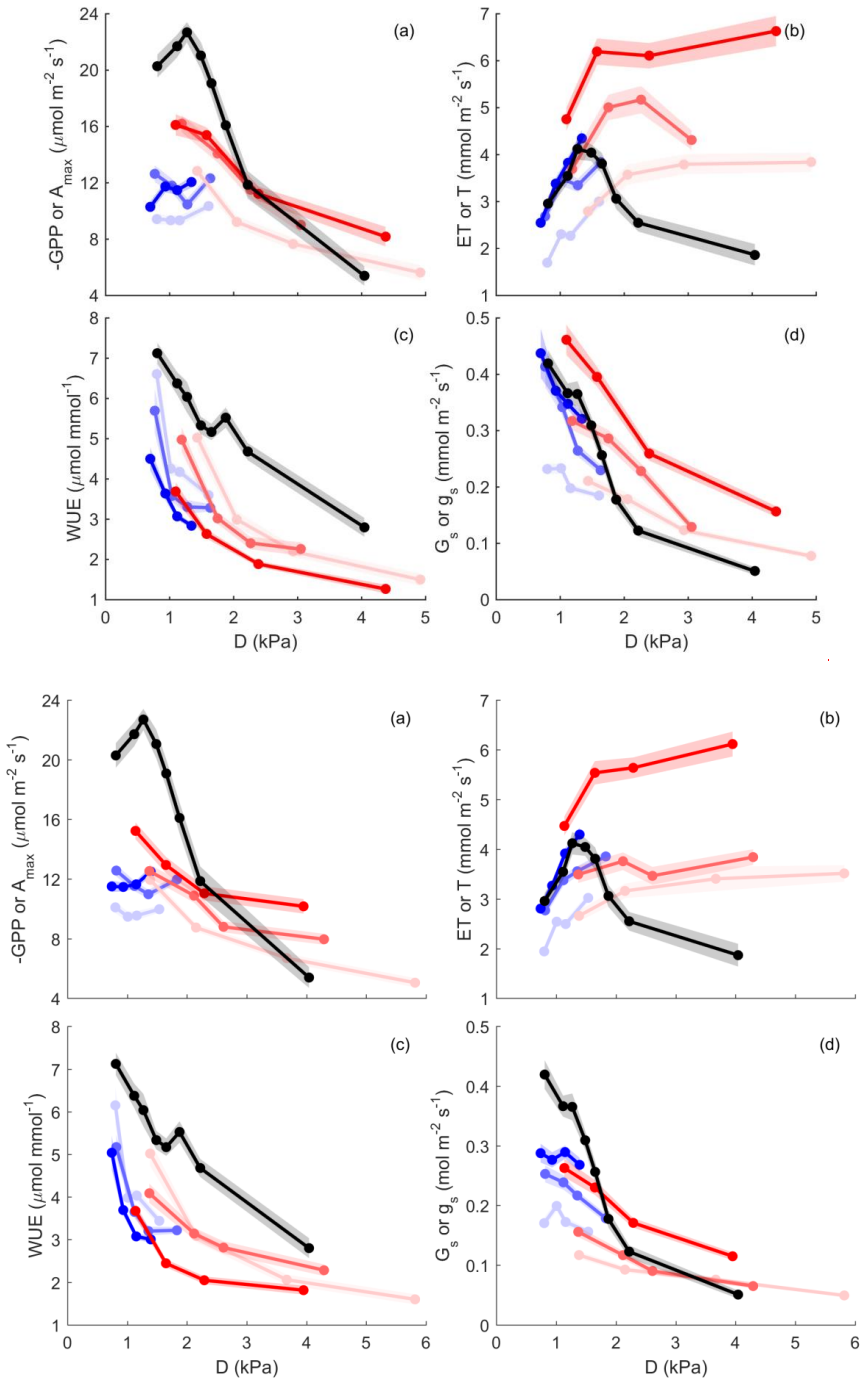

Figure 5 Gross primary productivity or net assimilation (GPP or Amax, µmol m^{-2} [ground or leaf] s^{-1}), evapotranspiration or leaf transpiration (ET or T, mmol m^{-2} [ground or leaf] s^{-1}), water use efficiency (WUE = GPP/ET or A_{max}/T, µmol mmol^{-1}) and surface conductance or leaf conductance (G_s or g_s, mmol m^{-2} s^{-1}) vs. vapour pressure deficit (D). Leaf level is shown in black, ecosystem scale is shown in color; summer (red) and winter (blue), at saturated ~~PAR~~PPFD (>1000 ~~W~~µmol m^{-2} s^{-1}). D is binned into 4 quartiles for ecosystem and 8 for leaf; Y is mean value for each D bins, plotted at the median of D bin.

562 Shaded area indicates the standard error of the mean. The three color intensity show SWC quantiles (SWC < 0.33, SWC
563 [0.33-0.67] and SWC [0.67-1.00] shown in decreasing color intensity).

564
565

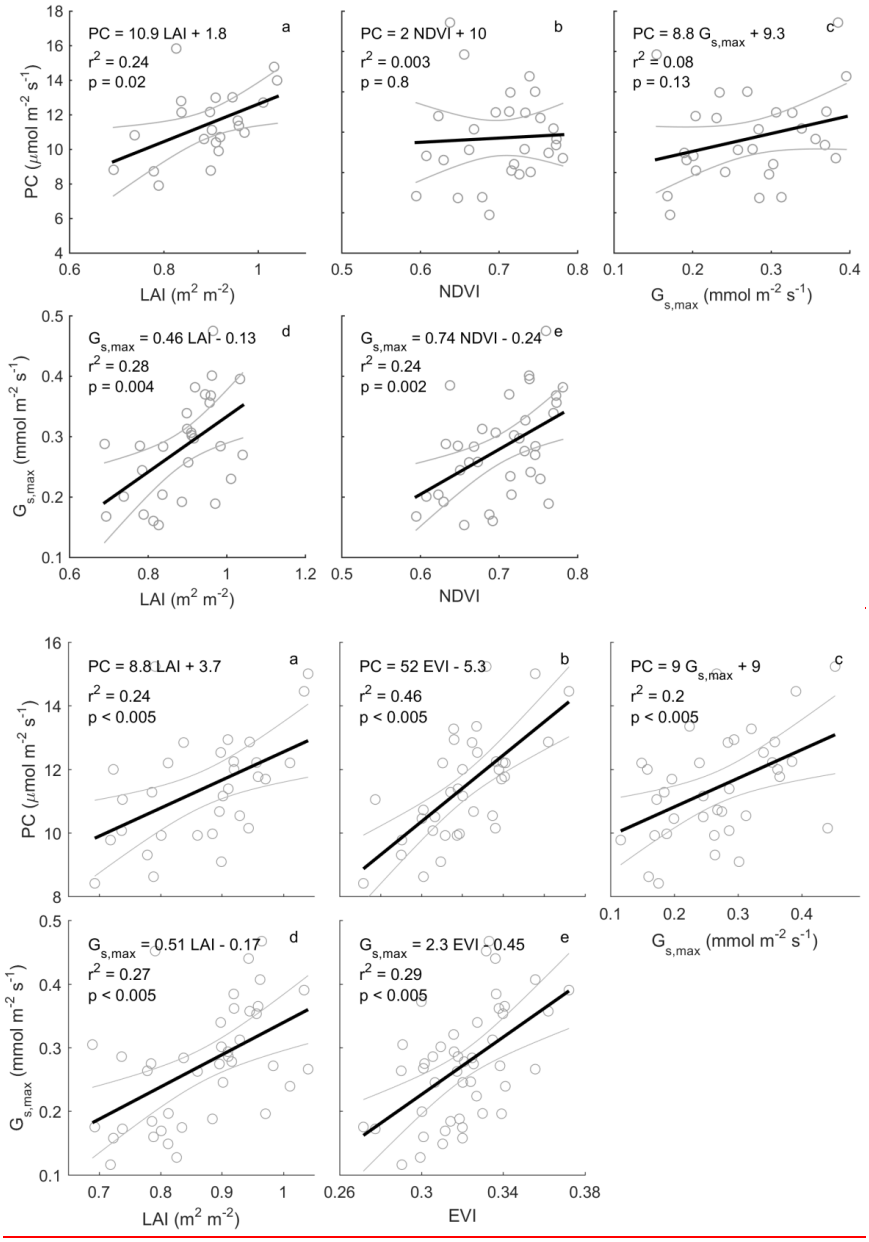

Figure 6 Relationships between monthly photosynthetic capacity (PC, µmol m^{-2} s^{-1}), leaf area index (LAI, m^2 m^{-2}), 250 m^2 ~~normalized~~enhanced vegetation index (~~NDVI~~EVI), and maximum surface conductance ($G_{s,max}$). Monthly PC / $G_{s,max}$ are calculated as the median / 75% quantile of half-hourly GPP / G_s when ~~PAR~~PPFD [800-1200 ~~W~~µmol m^{-2} s^{-1}] and D [1-1.5 kPa]; rain events are filtered for $G_{s,max}$ estimation, to minimise evaporation contribution to evapotranspiration (see methods). Monthly LAI is calculated as mean of LAI smoothed by a spline. Thick black line shows a linear regression. ~~PC vs. LAI was significant (r^2 = 0.58, p = 3.7e-05, slope = 20.1 ± 3.8). $G_{s,max}$ vs. LAI was also significant (r^2 = 0.28, p = 0.004, slope = 0.46 ± 0.15).~~ For PC calculation, GPP data is only used when quality-checked NEE is available (GPP = NEE measured – ER estimated by a neural network, see method).

Formatted: Caption

Formatted: Font color: Text 1

Table 1 Annual precipitation (P, mm y^{-1}), evapotranspiration (ET, mm y^{-1}), air temperature T_a (°C), net ecosystem exchange (NEE, g C m^{-2} y^{-1}), gross ecosystem production (GPP, g C m^{-2} y^{-1}) and ecosystem respiration (ER, g C m^{-2} y^{-1}) for the ~~three~~four year study period.

Period	P (mm y^{-1})	ET (mm y^{-1})	T_a (°C)	NEE (g C m^{-2} y^{-1})	GPP (g C m^{-2} y^{-1})	ER (g C m^{-2} y^{-1})
2014 all	**733**	**802797**	**18.4**	**-54124**	**-13471301**	**12931177**
~~winter~~Winter			12.81			
	149	142	3	-127145	-268265	141120
~~spring~~Spring	129	193189	19.3	-820	-355333	347313
Summer~~summer~~			22.82			
	279	275	3	9780	-338302	434382
~~autumn~~Autumn			18.81			
	176	192190	9	-1539	-385401	370362
2015 all	**978**	**935938**	**18.0**	**-183234**	**-16411517**	**14581283**
~~winter~~Winter	122	160	12.0	-135131	-322335	187204
~~spring~~Spring	237	223	19.1	-2843	-429392	401349
~~summer~~Summer	273	318	23.0	3124	-481426	512449
~~autumn~~Autumn	345	234238	18.1	-5184	-410365	359280
2016 all			**18.81**			
	893	**849852**	**9**	**-337372**	**-17351664**	**13981292**
~~winter~~Winter	335	161164	13.1	-99130	-283288	185158
~~spring~~Spring			18.81			
	96	208207	9	-135149	-469444	334295
~~summer~~Summer			23.72			
	412	308311	4	-158	-560524	545516
~~autumn~~Autumn			19.62			
	50	172171	0	-8885	-422408	334323
2017 all	**821**	**798**	**19**	**-171**	**-1486**	**1315**
Winter	139	148	13	-177	-329	152
Spring	85	178	19	-80	-383	303
Summer	194	236	25	78	-350	428
Autumn	403	237	18	8	-424	432

References

Aubinet, M., T. Vesala, and D. Papale, 2012: *Eddy Covariance A Practical Guide to Measurement and Data Analysis.* Springer.

Aubinet, M., B. Chermanne, B.,M. Vandenhaute, M.,B. Longdoz, B.,M. Yernaux, M., and E. Laitat, E.:2001: Long term carbon dioxide exchange above a mixed forest in the Belgian Ardennes.. *Agricultural and Forest Meteorology*, **108,** 293-315, 10.1016/s0168-1923(01)00244-1, 2001.

Aubinet, M., Vesala, T., and Papale, D.: Eddy Covariance A Practical Guide to Measurement and Data Analysis, edited by: Aubinet, M., Vesala, T., and Papale, D., Springer, 2012.

Baldocchi, D., Y. Ryu, Y., and T. Keenan, T.:2016: Terrestrial Carbon Cycle Variability.. *F1000Research*, **5**, 2016.

Baldocchi, D. D., B. B. Hicks, B. B., and T. P. Meyers, T. P.: Measuring biosphere-atmosphere exchanges of biologically related gases with micrometeorological methods,1988: MEASURING BIOSPHERE-ATMOSPHERE EXCHANGES OF BIOLOGICALLY RELATED GASES WITH MICROMETEOROLOGICAL METHODS. *Ecology*, **69,** 1331-1340, 10.2307/1941631, 1988.

Barr, A., Richardson, A., Hollinger, D., Papale, D., Arain, M., Black, T., Bohrer, G., Dragoni, D., Fischer, M., and Gu, L.:Barr, A., and Coauthors, 2013: Use of change-point detection for friction–velocity threshold evaluation in eddy-covariance studies.. *Agricultural and Forest Meteorology*, **171,** 31-45, 2013.

Beringer, J., Hutley, L. B., McHugh, I., Arndt, S. K., Campbell, D., Cleugh, H. A., Cleverly, J., de Dios, V. R., Eamus, D., Evans, B., Ewenz, C., Grace, P., Griebel, A., Haverd, V., Hinko-Najera, N., Huete, A., Isaac, P., Kanniah, K., Leuning, R., Liddell, M. J., Macfarlane, C., Meyer, W., Moore, C., Pendall, E., Phillips, A., Phillips, R. L., Prober, S. M., Restrepo-Coupe, N., Rutledge, S., Schroder, I., Silberstein, R., Southall, P., Yee, M. S., Tapper, N. J., van Gorsel, E., Vote, C., Walker, J., and Wardlaw, T.:Coauthors, 2016: An introduction to the Australian and New Zealand flux tower network - OzFlux.. *Biogeosciences*, **13,** 5895-5916, 10.5194/bg-13-5895-2016, 2016.

de Dios, V. R., Fellows, A. W., Nolan, R. H., Boer, M. M., Bradstock, R. A., Domingo, F., and Goulden, M. L.: A semi-mechanistic model for predicting the moisture content of fine litter, Agricultural and Forest Meteorology, 203, 64-73, 2015.

Breiman, L., 2001: Random forests. *Machine learning*, **45,** 5-32.

Dixon, R. K., S. Brown, S.,R. e. a. Houghton, R. e. a.,A. Solomon, A.,M. Trexler, M., and J. Wisniewski, J.:1994: Carbon pools and flux of global forest ecosystems.. *Science(Washington)*, **263,** 185-189, 1994.

Duursma, R. A., Barton, C. V., Lin, Y. S., Medlyn, B. E., Eamus, D., Tissue, D. T., Ellsworth, D. S., and McMurtrie, R. E.:Duursma, R. A., T. E. Gimeno, M. M. Boer, K. Y. Crous, M. G. Tjoelker, and D. S. Ellsworth, 2016: Canopy leaf area of a mature evergreen Eucalyptus woodland does not respond to elevated atmospheric CO2 but tracks water availability. *Global Change Biology*, **22,** 1666-1676.

Duursma, R. A., and Coauthors, 2014: The peaked response of transpiration rate to vapour pressure deficit in field conditions can be explained by the temperature optimum of photosynthesis.. *Agricultural and Forest Meteorology*, **189,** 2-10, 2014.

Duursma, R. A., Gimeno, T. E., Boer, M. M., Crous, K. Y., Tjoelker, M. G., and Ellsworth, D. S.: Canopy leaf area of a mature evergreen Eucalyptus woodland does not respond to elevated atmospheric CO2 but tracks water availability, Global Change Biology, 22, 1666-1676, 10.1111/gcb.13151, 2016.

Formatted: Font: Italic
Formatted: Font: Bold
Formatted: Font: Italic
Formatted: Font: Bold
Formatted: Font: Italic
Formatted: Font: Bold
Formatted: Font: Italic
Formatted: Font: Bold
Formatted: Font: Italic
Formatted: Font: Bold
Formatted: Font: Italic
Formatted: Font: Bold
Formatted: Font: Italic
Formatted: Font: Bold

Fan, S.-M., S. C. Wofsy, P. S. C., Bakwin, P. S.,D. J. Jacob, and D. J., andR. Fitzjarrald, D. R.:1990: Atmosphere-biosphere exchange of CO 2 and O 3 in the central Amazon forest, 1990.

Foken, T., 2008: The energy balance closure problem: an overview. *Ecological Applications*, **18,** 1351-1367.

Foken, T., F. Wimmer, M. Mauder, C. Thomas, and C. Liebethal, 2006: Some aspects of the energy balance closure problem. *Atmospheric Chemistry and Physics*, **6,** 4395-4402.

Foken, T., M. Gockede, M., Mauder, M.,L. Mahrt, L.,B. Amiro, B., and W. Munger, W.:2004: Post-field data quality control. *Handbook of Micrometeorology: A Guide for Surface Flux Measurement and Analysis*, **29,** 181-208, 2004.

Foken, T., Wimmer, F., Mauder, M., Thomas, C., and Liebethal, C.: Some aspects of the energy balance closure problem, Atmospheric Chemistry and Physics, 6, 4395-4402, 2006.

Foken, T.: The energy balance closure problem: an overview, Ecological Applications, 18, 1351-1367, 2008.

Gash, J., and A. Culf, A.:1996: Applying a linear detrend to eddy correlation data in realtime. *Boundary-Layer Meteorology*, **79,** 301-306, 1996.

Gimeno, T. E., Gimeno, T. E.,K. Y. Crous, K. Y.,J. Cooke, J., O'Grady, A. A. P. O'Grady, A. ,, Ósvaldsson, A.,B. E. Medlyn, B. E., and D. S. Ellsworth, D. S.:2016: Conserved stomatal behaviour under elevated CO2 and varying water availability in a mature woodland. *Functional Ecology*, **30,** 700-709, 2016.

Graham, E. A., S. S. Mulkey, S. S.,K. Kitajima, K.,N. G. Phillips, N. G., and S. J. Wright, S. J.:2003: Cloud cover limits net CO2 uptake and growth of a rainforest tree during tropical rainy seasons. *Proceedings of the National Academy of Sciences*, **100,** 572-576, 2003.

Griebel, A., D. M. Watson, and E. Pendall, 2017: Mistletoe, friend and foe: synthesizing ecosystem implications of mistletoe infection. *Environmental Research Letters*.

Griebel, A., L. T. Bennett, L. T.,D. S. Culvenor, D. S.,G. J. Newnham, G. J., and S. K. Arndt, S. K.:2015: Reliability and limitations of a novel terrestrial laser scanner for daily monitoring of forest canopy dynamics. *Remote Sensing of Environment*, **166,** 205-213, 2015.

Griebel, A., Watson, D. M., and Pendall, E.: Mistletoe, friend and foe: synthesizing ecosystem implications of mistletoe infection, Environmental Research Letters, 2017.

Hill, M. J., U. Senarath, U.,A. Lee, A.,M. Zeppel, J. M., Nightingale, R. D. J. M., Williams, R. D. J., and T. R. McVicar, T. R.:2006: Assessment of the MODIS LAI product for Australian ecosystems. *Remote Sensing of Environment*, **101,** 495-518, 2006.

Hinko-Najera, N., Isaac, P., Beringer, J., van Gorsel, E., Ewenz, C., McHugh, I., Exbrayat, J. F., Livesley, S. J., and Arndt, S. K.:and Coauthors, 2017: Net ecosystem carbon exchange of a dry temperate eucalypt forest. *Biogeosciences*, **14,** 3781-3800, 10.5194/bg-14-3781-2017, 2017.

Hsu, K. l., Gupta, H. V., Gao, X., Sorooshian, S., and Imam, B.: Self-organizing linear output map (SOLO): An artificial neural network suitable for hydrologic modeling and analysis, Water Resources Research, 38, 2002.

Hutyra, L. R., Munger, J. W., Saleska, S. R., Gottlieb, E., Daube, B. C., Dunn, A. L., Amaral, D. F., De Camargo, P. B., and Wofsy, S. C.:and Coauthors, 2007: Seasonal controls on the exchange of

Formatted: Font: Italic
Formatted: Font: Bold
Formatted: Font: Italic
Formatted: Font: Bold
Formatted: Font: Italic
Formatted: Font: Bold
Formatted: Font: Italic
Formatted: Font: Bold
Formatted: Font: Italic
Formatted: Font: Bold
Formatted: Font: Italic
Formatted: Font: Bold
Formatted: Font: Italic
Formatted: Font: Bold

carbon and water in an Amazonian rain forest~~.~~ *Journal of Geophysical Research: Biogeosciences*, **112**~~, 2007~~.

Isaac, P., J. Cleverly, ~~J.,~~I. McHugh, ~~I.,~~E. van Gorsel, ~~E.,~~C. Ewenz, ~~C.,~~ and J. Beringer, ~~J.:~~2017: OzFlux Data: Network integration from collection to curation~~.~~ *Biogeosciences*, **14,** 2903~~, 2017~~.

Jones, T. L., D. E. Tucker, and D. ~~E., and~~R. Ort, ~~D. R.:~~1998: Chilling delays circadian pattern of sucrose phosphate synthase and nitrate reductase activity in tomato~~.~~ *Plant Physiology*, **118,** 149-158~~, 1998~~.

Karan, M., ~~Liddell, M., Prober, S. M., Arndt, S., Beringer, J., Boer, M., Cleverly, J., Eamus, D., Grace, P.,~~ and ~~Van Gorsel, E.:~~Coauthors, 2016: The Australian Supersite Network: a continental, long-term terrestrial ecosystem observatory~~.~~ *Science of the Total Environment*, **568,** 1263-1274~~, 2016~~.

Keeling, C. D., S. C. Piper, ~~S. C.,~~R. B. Bacastow, ~~R. B.,~~M. Wahlen, ~~M.,~~T. P. Whorf, ~~T. P.,~~M. Heimann, ~~M.,~~ and H. A. Meijer, ~~H. A.:~~2001: Exchanges of atmospheric CO2 and 13CO2 with the terrestrial biosphere and oceans from 1978 to 2000. I. Global aspects~~.~~ *Scripps Institution of Oceanography*~~, 2001~~.

Keith, H., E. van Gorsel, ~~E.,~~K. L. Jacobsen, ~~K. L.,~~ and H. A. Cleugh, ~~H. A.:~~2012: Dynamics of carbon exchange in a Eucalyptus forest in response to interacting disturbance factors~~.~~ *Agricultural and Forest Meteorology*, **153,** 67-81~~, 10.1016/j.agrformet.2011.07.019, 2012~~.

~~Kljun, N., Calanca, P., Rotach, M. W., and Schmid, H. P.: A simple parameterisation for flux footprint predictions, Boundary-Layer Meteorology, 112, 503-523, 10.1023/b:boun.0000030653.71031.96, 2004.~~

Knauer, J., C. Werner, ~~C.,~~ and S. Zaehle, ~~S.:~~2015: Evaluating stomatal models and their atmospheric drought response in a land surface scheme: A multibiome analysis~~.~~ *Journal of Geophysical Research: Biogeosciences*, **120,** 1894-1911~~, 2015~~.

Knauer, J., ~~Zaehle, S., Medlyn, B. E., Reichstein, M., Williams, C. A., Migliavacca, M., De Kauwe, M. G., Werner, C., Keitel, C.,~~ and ~~Kolari, P.:~~Coauthors, 2017: Towards physiologically meaningful water-use efficiency estimates from eddy covariance data~~.~~ *Global Change Biology*~~, 2017~~.

Kolari, P., H. K. Lappalainen, H. ~~K.,~~ Hänninen, ~~H.,~~ and P. Hari, ~~P.:~~2007: Relationship between temperature and the seasonal course of photosynthesis in Scots pine at northern timberline and in southern boreal zone~~.~~ *Tellus B*, **59,** 542-552~~, 2007~~.

Kormann, R., and F. X. Meixner, 2001: An analytical footprint model for non-neutral stratification. *Boundary-Layer Meteorology*, **99,** 207-224.

Lim, P. O., H. J. Kim, ~~H. J.,~~ and H. Gil Nam, ~~H.:~~2007: Leaf senescence~~.~~ *Annu. Rev. Plant Biol.*, **58,** 115-136~~, 2007~~.

Lindroth, A., L. Klemedtsson, ~~L.,~~A. Grelle, ~~A.,~~P. Weslien, ~~P.,~~ and O. Langvall, ~~O.:~~2008: Measurement of net ecosystem exchange, productivity and respiration in three spruce forests in Sweden shows unexpectedly large soil carbon losses~~.~~ *Biogeochemistry*, **89,** 43-60~~, 2008~~.

Lloyd, J., and J. A. Taylor, ~~J. A.: On the temperature dependence of soil respiration,~~1994: ON THE TEMPERATURE-DEPENDENCE OF SOIL RESPIRATION. *Functional Ecology*, **8,** 315-323~~, 10.2307/2389824, 1994~~.

Formatted: Font: Italic
Formatted: Font: Bold

Medlyn, B. E., Duursma, R. A., Eamus, D., Ellsworth, D. S., Prentice, I. C., Barton, C. V. M., Crous, K. Y., De Angelis, P., Freeman, M., and Wingate, L.:Coauthors, 2011: Reconciling the optimal and empirical approaches to modelling stomatal conductance., *Global Change Biology*, **17,** 2134-2144, 10.1111/j.1365-2486.2010.02375.x, 2011.

Mitscherlich, E. A.:., 1909: Das Gesetz des Minimums und das Gesetz des abnehmenden Bodenertrages., *Landw. Jahrb*, **38,** 537-552, 1909.

Moncrieff, J., R. Clement, R.,J. Finnigan, J., and T. Meyers, T.:2004: Averaging, detrending, and filtering of eddy covariance time series, in:, *Handbook of micrometeorology*, Springer, 7-31, 2004.

Moncrieff, J. B., Massheder, J. M., deBruin, H., Elbers, J., Friborg, T., Heusinkveld, B., Kabat, P., Scott, S., Soegaard, H., and Verhoef, A.:Coauthors, 1997: A system to measure surface fluxes of momentum, sensible heat, water vapour and carbon dioxide., *Journal of Hydrology*, **189,** 589-611, 1997.

Monteith, J. L.:., 1965: Evaporation and environment., *Symp. Soc. Exp. Biol*, 1965, 4, .

Moore, C. E., T. F. Keenan, T. F.,R. A. Duursma, R. A., I. van Dijk, A. I.,L. B. Hutley, L. B.,J. R. Taylor, J. R., and M. J. Liddell, M. J.:2016: Reviews and syntheses: Australian vegetation phenology: new insights from satellite remote sensing and digital repeat photography., *Biogeosciences*, **13,** 5085, 2016.

Munné-Bosch, S., and L. Alegre, L.:2004: Die and let live: leaf senescence contributes to plant survival under drought stress., *Functional Plant Biology*, **31,** 203-216, 2004.

Novick, K. A., A. C. Oishi, A. C.,E. J. Ward, E. J.,M. B. S. Siqueira, M. B. S.,J. Y. Juang, J. Y., and P. C. Stoy, P. C.:2015: On the difference in the net ecosystem exchange of CO2 between deciduous and evergreen forests in the southeastern United States., *Global Change Biology*, **21,** 827-842, 10.1111/gcb.12723, 2015.

Novick, K. A., Ficklin, D. L., Stoy, P. C., Williams, C. A., Bohrer, G., Oishi, A. C., Papuga, S. A., Blanken, P. D., Noormets, A., Sulman, B. N., Scott, R. L., Wang, L. X., and Phillips, R. P.:Coauthors, 2016: The increasing importance of atmospheric demand for ecosystem water and carbon fluxes., *Nature Climate Change*, **6,** 1023-1027, 10.1038/nclimate3114, 2016.

Pan, Y., Birdsey, R. A., Fang, J., Houghton, R., Kauppi, P. E., Kurz, W. A., Phillips, O. L., Shvidenko, A., Lewis, S. L., and Canadell, J. G.:Coauthors, 2011: A large and persistent carbon sink in the world's forests., *Science*, **333,** 988-993, 2011.

Pook, E.:., 1984: Canopy dynamics of Eucalyptus maculata Hook. II. Canopy leaf area balance., *Australian Journal of Botany*, **32,** 405-413, 1984.

Poulter, B., Frank, D., Ciais, P., Myneni, R. B., Andela, N., Bi, J., Broquet, G., Canadell, J. G., Chevallier, F., Liu, Y. Y., Running, S. W., Sitch, S., and van der Werf, G. R.:Coauthors, 2014: Contribution of semi-arid ecosystems to interannual variability of the global carbon cycle., *Nature*, **509,** 600-603, 10.1038/nature13376, 2014.

Prior, L. D., and D. M. Bowman, D. M.:2014: Big eucalypts grow more slowly in a warm climate: evidence of an interaction between tree size and temperature., *Global change biology*, **20,** 2793-2799, 2014.

Reich, P. B., D. S. Falster, D. S. Ellsworth, I. J. Wright, M. Westoby, J. Oleksyn, and T. D. Lee, 2009: Controls on declining carbon balance with leaf age among 10 woody species in Australian woodland: do leaves have zero daily net carbon balances when they die? *New Phytologist*, **183,** 153-166.

Formatted: Font: Italic
Formatted: Font: Bold

Resco de Dios, V., A. W. Fellows, R. H. Nolan, M. M. Boer, R. A. Bradstock, F. Domingo, and M. L. Goulden, 2015: A semi-mechanistic model for predicting the moisture content of fine litter. *Agricultural and Forest Meteorology*, **203,** 64-73.

Restrepo-Coupe, N., ~~Huete, A., Davies, K., Cleverly, J., Beringer, J., Eamus, D., Gorsel, E. v., Hutley, L. B., and Meyer, W. S.:~~and Coauthors, 2016: MODIS vegetation products as proxies of photosynthetic potential along a gradient of meteorologically and biologically driven ecosystem productivity~~.~~. *Biogeosciences*, **13,** 5587-5608~~, 2016~~.

Restrepo-Coupe, N., ~~Levine, N. M., Christoffersen, B. O., Albert, L. P., Wu, J., Costa, M. H., Galbraith, D., Imbuzeiro, H., Martins, G.,~~ and ~~Araujo, A. C.:~~Coauthors, 2017: Do dynamic global vegetation models capture the seasonality of carbon fluxes in the Amazon basin? A data-model intercomparison~~.~~. *Global change biology*, **23,** 191-208~~, 2017~~.

Saleska, S. R., ~~Miller, S. D., Matross, D. M., Goulden, M. L., Wofsy, S. C., Da Rocha, H. R., De Camargo, P. B., Crill, P., Daube, B. C.,~~ and ~~De Freitas, H. C.:~~Coauthors, 2003: Carbon in Amazon forests: unexpected seasonal fluxes and disturbance-induced losses~~.~~. *Science*, **302,** 1554-1557~~, 2003~~.

Schimel, D. S., ~~House, J. I., Hibbard, K. A., Bousquet, P., Ciais, P., Peylin, P., Braswell, B. H., Apps, M. J., Baker, D.,~~ and ~~Bondeau, A.:~~Coauthors, 2001: Recent patterns and mechanisms of carbon exchange by terrestrial ecosystems~~.~~. *Nature*, **414,** 169-172~~, 2001~~.

Thom, A.~~:~~., 1972: Momentum, mass and heat exchange of vegetation~~.~~. *Quarterly Journal of the Royal Meteorological Society*, **98,** 124-134~~, 1972~~.

Tjoelker, M. G., J. Oleksyn, ~~J.,~~ and P. B. Reich, ~~P. B.:~~2001: Modelling respiration of vegetation: evidence for a general temperature-dependent Q10~~.~~. *Global Change Biology*, **7,** 223-230~~, 2001~~.

Trenberth, K. E.~~:~~., 1983: What are the seasons~~?~~.? *Bulletin of the American Meteorological Society*, **64,** 1276-1282~~, 1983~~.

~~van Gorsel, E., Berni, J. A. J., Briggs, P., Cabello-Leblic, A., Chasmer, L., Cleugh, H. A., Hacker, J., Hantson, S., Haverd, V., Hughes, D., Hopkinson, C., Keith, H., Kljun, N., Leuning, R., Yebra, M., and Zegelin, S.:~~van Gorsel, E., and Coauthors, 2013: Primary and secondary effects of climate variability on net ecosystem carbon exchange in an evergreen Eucalyptus forest~~.~~. *Agricultural and Forest Meteorology*, **182-183,** 248-256~~, 10.1016/j.agrformet.2013.04.027, 2013~~.

Vickers, D., and L. Mahrt, ~~L.:~~1997: Quality control and flux sampling problems for tower and aircraft data~~.~~. *Journal of Atmospheric and Oceanic Technology*, **14,** 512-526~~, 1997~~.

Webb, E. K., G. I. Pearman, ~~G. I.,~~ and R. Leuning, ~~R.:~~1980: Correction of flux measurements for density effects due to heat and water vapour transfer~~.~~. *Quarterly Journal of the Royal Meteorological Society*, **106,** 85-100~~, 1980~~.

Wilczak, J. M., S. P. Oncley, ~~S. P.,~~ and S. A. Stage, ~~S. A.:~~2001: Sonic anemometer tilt correction algorithms~~.~~. *Boundary-Layer Meteorology*, **99,** 127-150~~, 2001~~.

Wilson, K., ~~Goldstein, A., Falge, E., Aubinet, M., Baldocchi, D., Berbigier, P., Bernhofer, C., Ceulemans, R., Dolman, H.,~~ and ~~Field, C.:~~Coauthors, 2002: Energy balance closure at FLUXNET sites~~.~~. *Agricultural and Forest Meteorology*, **113,** 223-243~~, 2002~~.

Wilson, K. B., ~~Baldocchi,~~D. D. ~~D.,~~Baldocchi, and P. J. Hanson, ~~P. J.:~~2001: Leaf age affects the seasonal pattern of photosynthetic capacity and net ecosystem exchange of carbon in a deciduous forest~~.~~. *Plant Cell and Environment*, **24,** 571-583~~, 10.1046/j.0016-8025.2001.00706.x, 2001~~.

Formatted: Font: Italic
Formatted: Font: Bold
Formatted: Font: Italic
Formatted: Font: Bold
Formatted: Font: Italic
Formatted: Font: Bold
Formatted: Font: Italic
Formatted: Font: Bold
Formatted: Font: Italic
Formatted: Font: Bold
Formatted: Font: Italic
Formatted: Font: Bold
Formatted: Font: Italic
Formatted: Font: Bold
Formatted: Font: Italic
Formatted: Font: Bold
Formatted: Font: Italic
Formatted: Font: Bold
Formatted: Font: Italic
Formatted: Font: Bold
Formatted: Font: Italic
Formatted: Font: Bold
Formatted: Font: Italic
Formatted: Font: Bold
Formatted: Font: Italic
Formatted: Font: Bold

Windsor, D. M.:., 1990: Climate and moisture variability in a tropical forest: long-term records from Barro Colorado Island, Panama, 1990.

Wu, J., Albert, L. P., Lopes, A. P., Restrepo-Coupe, N., Hayek, M., Wiedemann, K. T., Guan, K. Y., Stark, S. C., Christoffersen, B., Prohaska, N., Tavares, J. V., Marostica, S., Kobayashi, H., Ferreira, M. L., Campos, K. S., da Silva, R., Brando, P. M., Dye, D. G., Huxman, T. E., Huete, A. R., Nelson, B. W., and Saleska, S. R.:Coauthors, 2016: Leaf development and demography explain photosynthetic seasonality in Amazon evergreen forests., *Science*, **351,** 972-976, 10.1126/science.aad5068, 2016.

Xia, J. Y., Niu, S. L., Ciais, P., Janssens, I. A., Chen, J. Q., Ammann, C., Arain, A., Blanken, P. D., Cescatti, A., Bonal, D., Buchmann, N., Curtis, P. S., Chen, S. P., Dong, J. W., Flanagan, L. B., Frankenberg, C., Georgiadis, T., Gough, C. M., Hui, D. F., Kiely, G., Li, J. W., Lund, M., Magliulo, V., Marcolla, B., Merbold, L., Montagnani, L., Moors, E. J., Olesen, J. E., Piao, S. L., Raschi, A., Roupsard, O., Suyker, A. E., Urbaniak, M., Vaccari, F. P., Varlagin, A., Vesala, T., Wilkinson, M., Weng, E., Wohlfahrt, G., Yan, L. M., and Luo, Y. Q.:Coauthors, 2015: Joint control of terrestrial gross primary productivity by plant phenology and physiology., *Proceedings of the National Academy of Sciences of the United States of America*, **112,** 2788-2793, 10.1073/pnas.1413090112, 2015.

Yi, C., Ricciuto, D., Li, R., Wolbeck, J., Xu, X., Nilsson, M., Aires, L., Albertson, J. D., Ammann, C., and Arain, M. A.:Coauthors, 2010: Climate control of terrestrial carbon exchange across biomes and continents., *Environmental Research Letters*, **5,** 034007, 2010.

Zhang, Y., Z. Tan, Z.,Q. Song, Q.,G. Yu, G., and X. Sun, X.:2010: Respiration controls the unexpected seasonal pattern of carbon flux in an Asian tropical rain forest., *Atmospheric Environment*, **44,** 3886-3893, 2010.

Formatted: Font: Italic
Formatted: Font: Bold
Formatted: Font: Italic
Formatted: Font: Bold
Formatted: Font: Italic
Formatted: Font: Bold
Formatted: Font: Italic
Formatted: Font: Bold